Available online at www.sciencedirect.com
SCIENCE DIRECT®
Biochemical and Biophysical Research Communications 323 (2004) 218–222
BBRC
www.elsevier.com/locate/ybbrc

Cellular prion protein regulates intracellular hydrogen peroxide level and prevents copper-induced apoptosis

Takuya Nishimura[a], Akikazu Sakudo[a], Izuru Nakamura[a], Deug-chan Lee[a], Yojiro Taniuchi[a], Keiichi Saeki[a], Yoshitsugu Matsumoto[a], Masaharu Ogawa[b], Suehiro Sakaguchi[d], Shigeyoshi Itohara[c], Takashi Onodera[a,*]

[a] *Department of Molecular Immunology, School of Agricultural and Life Sciences, University of Tokyo, Bunkyo-ku, Tokyo 113-8657, Japan*
[b] *Laboratory for Cell Culture Development, Brain Science Institute, RIKEN, Wako, Saitama 351-0198, Japan*
[c] *Laboratory for Behavioral Genetics, Brain Science Institute, RIKEN, Wako, Saitama 351-0198, Japan*
[d] *Department of Molecular Microbiology and Immunology, Nagasaki University, Graduate School of Biomedical Science, Sakamoto, Nagasaki 852-8523, Japan*

Received 11 August 2004
Available online 28 August 2004

Abstract

The function of cellular prion protein (PrP^C), which is a copper binding protein, remains unclear. To elucidate the mechanisms in which PrP^C is involved in neuroprotection, we compared death signals in prion protein gene-deficient ($Prnp^{-/-}$) primary cerebellar granular neurons (CGNs) to those with wild-type (WT) CGNs. When copper was exposed to these CGNs, ZrchI, and Rikn $Prnp^{-/-}$ CGNs were more sensitized and underwent apoptotic cell death more readily than WT CGNs. Furthermore, the level of intracellular hydrogen peroxide (H_2O_2) in WT CGNs increased by copper toxicity, whereas those in ZrchI and Rikn $Prnp^{-/-}$ CGNs did not. These results suggest that PrP^C modulates the intracellular H_2O_2 level as a copper-binding protein to protect CGNs from apoptotic cell death possibly due to inhibiting a Fenton reaction.

Keywords: Prion protein; PrP-deficient mouse; Copper; Cerebellar granular neurons

The fundamental physiological function of native cellular prion protein (PrP^C) remains unknown. There are several experimental findings related to the prion protein (PrP) function. A considerable amount of data has been accumulated on the response to oxidative stress [1]. In this study, we elucidated the neuroprotective properties of PrP^C in response to copper (Cu) and oxidative stress in the physiological aspect of PrP^C.

PrP^C deficiency results in neuronal phenotypes sensitive to oxidative stress induced by superoxide anion and hydrogen peroxide (H_2O_2) [1–3]. ZrchI PrP gene-deficient ($Prnp^{-/-}$) cerebellar neurons show increased sensitivity to superoxide anion generated by xanthine/xanthine oxidase [2]. Increased sensitivity of ZrchI $Prnp^{-/-}$ neurons to H_2O_2-induced cell death is evident compared to wild-type (WT) neurons [3]. The fact that ZrchI $Prnp^{-/-}$ neurons display lower glutathione reductase (GR) activity, breakdown of H_2O_2 is therefore inhibited [3]. ZrchI $Prnp^{-/-}$ neurons are more sensitive to Cu than WT neurons [4]. Additional neuroprotective effects of PrP have been observed when immortalized neuronal cell lines from Rikn $Prnp^{-/-}$ hippocampal cells are more apoptosis-susceptible to serum withdrawal than WT counterparts [5]. In addition, PrP^C inhibits Bax-induced apoptosis in the primary culture of human neurons [6]. Deletion of the octapeptide repeat domain abolishes this neuroprotective function of PrP^C, and elimination of the glycosyl phosphatidylinositol (GPI)-anchoring sequences elicits no protective effects [6]. Removal of

* Corresponding author. Fax: +81 3 5841 8020.
E-mail address: aonoder@mail.ecc.u-tokyo.ac.jp (T. Onodera).

0006-291X/$ - see front matter © 2004 Elsevier Inc. All rights reserved.
doi:10.1016/j.bbrc.2004.08.087

serum from neuronal cultures and Bax expression are known to induce intracellular oxidative stress [7,8], and the role of PrP^C in modulating neuronal antioxidant homeostasis has thus been suggested. Prion-infected GT1-7 cells significantly raise the levels of lipid peroxidation, increase sensitivity to glutathione depletion, and attenuate Cu, Zn-superoxide dismutase (SOD), Mn-SOD, GR, and glutathione peroxidase activities [9]. The amounts of lipid and protein oxidation in the brain tissues of *Prnp*$^{-/-}$ mice increase simultaneously, accompanied by decreased SOD activities [10,11]. Despite such significant evidence supporting a neuroprotective role of PrP^C against oxidative stress, the mediatory roles of PrP^C in neuroprotection are still unknown.

Cu binds to PrP at a major Cu(II)-binding site identified as the N-terminal domain; viz., a specific octapeptide region with four sequential repeats [12,13]. PrP^C has a direct role in brain Cu metabolism, with protein-transporting Cu(II) ions from the extracellular milieu acidifying the cellular vacuoles [14]. Contrary to these findings, a recent study has concluded that PrP^C does not participate in the uptake of extracellular Cu(II) at physiological concentrations of Cu [15]. The total brain Cu content in ZrchI *Prnp*$^{-/-}$ mice is not significantly different from that in WT mice [16,17]. In vitro experiments using recombinant mouse and chicken PrP^C refolding to corporate Cu(II) have revealed that PrP^C displays SOD activity [18], which is dependent on the Cu level incorporated into the molecule [18]. Although actual mechanisms of the PrP-related dismutase reaction remain unknown as yet, findings have suggested that neurodegenerative disorders in prion diseases may be caused by abnormalities in Cu metabolism.

Extensive overlaps between systems controlling homeostasis of redox-active metals such as Cu, iron, and oxygen radical metabolisms have been documented [19]. However, the biochemical mechanisms underlying the Cu-induced apoptosis are poorly understood. In this study, we investigated the mechanisms underlying the Cu-induced apoptosis in the primary culture of ZrchI and Rikn *Prnp*$^{-/-}$ cerebellar granular neurons (CGNs). The abnormalities of ZrchI and Rikn *Prnp*$^{-/-}$ CGNs and the mechanisms of neuroprotective effect of PrP^C were analyzed. This study shows that PrP^C regulates the intracellular H_2O_2 level after binding to Cu molecules to prevent neuronal death.

Materials and methods

Animals. ZrchI *Prnp*$^{-/-}$ mice [20] and Rikn *Prnp*$^{-/-}$ mice [21] were used in this study. C57BL/6CrSlc (WT) mice were purchased from Nippon SLC (Hamamastu, Japan).

Reagents. Unless otherwise specified, chemical reagents were obtained from Sigma (St. Louis, MO) and Wako Pure Chemical (Osaka, Japan).

Neuronal cell culture. CGNs were isolated from 6-day-old mice. Following dissociation in Hanks' balanced salt solution and digestion in 0.5% trypsin, cerebella were plated at $1–2 \times 10^6$ cells/cm^2 in poly-L-lysine (PLL) coated dishes (Falcon). Cultures were maintained in Neurobasal media (NB; Gibco) supplemented with B27, 25 mM KCl, 2 mM glutamine, and 1% antibiotics (penicillin, streptomycin). Cultures were maintained at 37 °C in atmosphere with 5% CO_2.

Cell viability was determined on the last day of the experiments. In brief, 3-(4,5-dimetyl-thiazol-2-yl)-2,5 diphenyl-tetrazolium bromide (MTT) was diluted to 200 μM and added to cultures for 2 h at 37 °C. The MTT-formazan product was released from cells by adding isopropanol before being measured by 570-nm spectrophotometry. Survival ratios compared to non-treated controls were determined.

Detection of apoptosis. DNA fragmentation was detected by the DNA ladder assay [22]. Harvested cells were prepared with lysis using lysis buffer [10 mM Tris–HCl (pH 7.4), 10 mM EDTA (pH8.0), and 0.5% Triton X-100] for 20 min on ice before centrifugation (12,000*g*, 30 min). The aqueous phase was incubated with 400 μg/ml DNase-free RNase A (Nippongene, Tokyo Japan) for 1 h at 37 °C. Proteins were digested with 400 μg/ml proteinase K for 1 h at 37 °C before DNA was precipitated overnight in aqueous 0.4 M NaCl containing 50% isopropanol at −20 °C. Precipitated DNA samples were resuspended in TE buffer and electrophoresed in 2% agarose gel. The gel was stained with ethidium bromide (0.5 μg/ml) for 10 min and destained with ultra-purified water for 10 min. DNA bands visualized by a UV light transilluminator were photographed (Bio-Rad, Cambridge, MA) accordingly.

Nuclear morphological analysis. Apoptosis was assessed by staining cell nuclei with 4′,6-diamino-2-phenylindole dihydrochloride (DAPI; Dojindo, Kumamoto, Japan) based on methods adapted from those previously described [23]. Cells with degenerating nuclei were thus discriminated. Briefly, cells were fixed for 20 min in fresh 4% paraformaldehyde in PBS(−), rinsed with PBS(−), before staining for 15 min with 3 μM DAPI in PBS(−). After being washed twice, cells were scored for chromatin condensation by fluorescence microscopy using a fluorescein filter (330–380 nm excitation). Total and apoptotic nuclei were counted. In all cases, >100 cells were counted per well. At least three different cell cultures utilizing four separate wells were employed.

PrP^C expression by flowcytometry. To examine PrP^C expression, flowcytometry was used as previously described [22]. Briefly, collected cells were initially incubated with 6H4 antibody (Prionics, Zurich, Switzerland) as the primary antibody and detected with FITC-labeled secondary antibody before analysis with a flowcytometer (FACScan).

Measurement of intracellular H_2O_2. Intracellular H_2O_2 levels were determined based on methods adapted from those previously described [24,25]. Cells were seeded in 6-cm culture dishes at 1×10^5 cells/well. Cells were incubated in various conditions. After the incubation, the cells were loaded with a final concentration of 10 μM of 2′7′-dichlorofluorescein diacetate (DCFH-DA) (Lambda Fluoreszenztechnologie, Graz, Austria) delivered in serum-free media for 15 min at 37 °C. DCFH-DA was incorporated into viable cells and hydrolyzed by intracellular elastase, generating the non-fluorescent molecule DCFH. Intercellular H_2O_2 oxidized DCFH to yield the fluorescent DCF molecule. Cells collected by pipetting without washing were subsequently analyzed. The fluorescence of each well was measured by a flowcytometer (480 nm excitation and 530 nm emission wavelengths). The total number of events was >5000 per sample.

Statistical analysis. Individual cultures were performed in triplicate. The results expressed as the means ± SEM for the number of culture preparations are indicated in the respective figures. Statistical analysis of results was performed by the non-paired Student's *t*-test. In cases where $p < 0.05$, the differences were considered significant.

Results and discussion

Previous study has shown that ZrchI *Prnp*$^{-/-}$ cerebellar cells are more sensitive to Cu toxicity than WT

cerebellar cells [4]. To further characterize the cell death in *Prnp*$^{-/-}$ cells exposed to Cu, the differences of DNA fragmentation in apoptosis between Rikn *Prnp*$^{-/-}$ and WT CGNs were examined. Rikn *Prnp*$^{-/-}$ and WT CGNs were cultured in $CuCl_2$ containing media (NB/B27) for 48 h, and samples were analyzed by DNA ladder assay. Exposure of Cu to CGNs showed significantly more cell deaths in *Prnp*$^{-/-}$ neurons compared with WT CGNs. The exposure of cultivated cells to 100–300 μM Cu resulted in more apoptotic cell death in Rikn *Prnp*$^{-/-}$ CGNs than WT CGNs (Fig. 1A). The CGN viability was assayed by the normal and apoptotic (condensed and fragmented) DAPI-stained nuclei were counted under fluorescence microscopy. More than 70% of Rikn *Prnp*$^{-/-}$ CGNs and less than 40% of WT CGNs incubated for 24 h in Cu (300 μM)-containing media showed bright pyknotic soma with disintegrated neurite under phase-contrast microscopy (data not shown), and ca. 80% of Rikn *Prnp*$^{-/-}$ CGNs and ca. 50% of WT CGNs exhibited condensed or fragmented nuclei when stained with DAPI, manifesting typical features of apoptosis (Fig. 1B).

Of Cu toxicities observed in WT, Zrchl *Prnp*$^{-/-}$, and Rikn *Prnp*$^{-/-}$ CGNs in NB/B27, the Zrchl and Rikn *Prnp*$^{-/-}$ CGNs were more sensitive than WT CGNs (Fig. 2). Cu-containing media were significantly more toxic to Zrchl and Rikn *Prnp*$^{-/-}$ CGNs than WT CGNs after 48-h exposure at 150 and 200 μM (Fig. 2). Next, as Cu is a redox active metal in a Fenton reaction, which produces hydroxyl radicals from H_2O_2, intracellular H_2O_2 was monitored to ascertain if Cu was involved in a Fenton

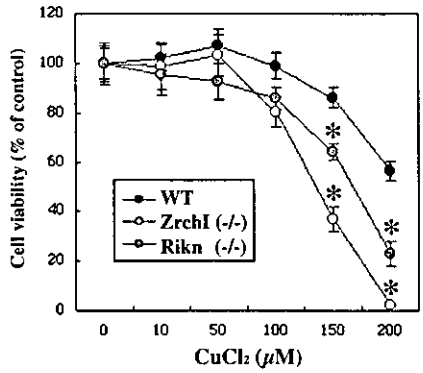

Fig. 2. Effect of Cu on cell viability in primary cultures of wild-type (WT), Zrchl and Rikn *Prnp*$^{-/-}$ cerebellar granular neurons (CGNs). Seven-day-old primary CGNs of WT, Zrchl, and Rikn *Prnp*$^{-/-}$ mice were exposed to $CuCl_2$ for 48 h, respectively, and cell viabilities were then determined using the MTT assay. Zrchl and Rikn *Prnp*$^{-/-}$ CGNs in NB/B27 medium were significantly more susceptible to 150 and 200 μM $CuCl_2$ toxicity than WT CGNs after 48-h exposure. Differences where $p < 0.05$ (*) were significant when compared with WT CGNs.

reaction-mediated cell damage in WT, Zrchl or Rikn *Prnp*$^{-/-}$ CGNs. By means of fluorochrome DCFH-DA coupled with flowcytometric technique, the level of intracellular H_2O_2 was monitored. Cu-treated WT CGNs increased H_2O_2 in a time-dependent manner with the peak established at 5 h after Cu-exposure (Fig. 3), whereas, at any tested time or concentration, signals indicating H_2O_2 increases were not detected in Zrchl and Rikn *Prnp*$^{-/-}$ CGNs. This finding indicated that the H_2O_2 production of WT CGNs was more highly induced by Cu

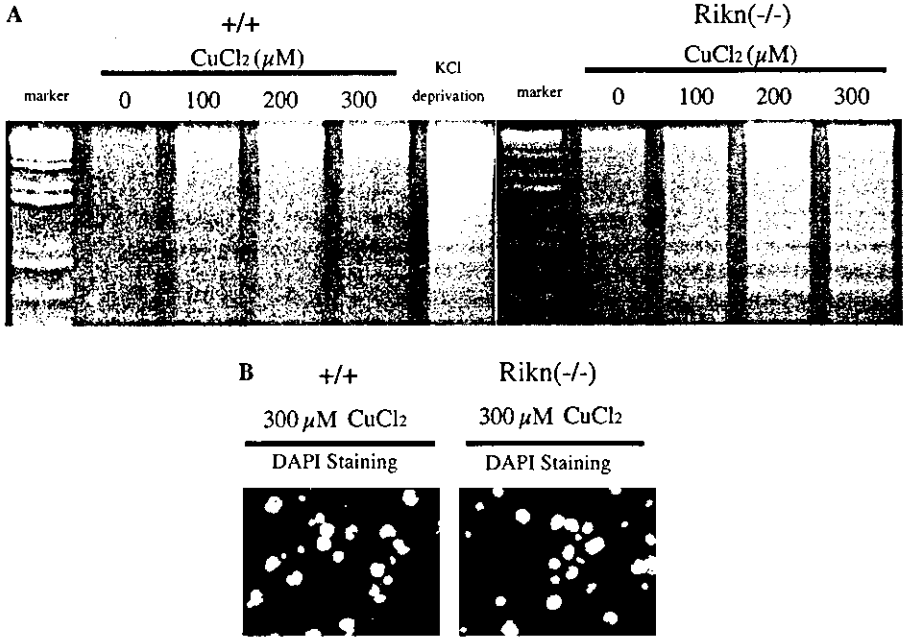

Fig. 1. Detection of Cu-induced apoptosis in WT and *Prnp*$^{-/-}$ cerebral granular neurons (CGNs). (A) CGNs derived from WT and Rikn *Prnp*$^{-/-}$ mice were cultured in media with the indicated concentrations of $CuCl_2$ or 5 mM KCl for 48 h and analyzed by the DNA fragmentation assay. (B) Alteration in nuclear morphology was visualized by DAPI staining after incubation of WT and Rikn *Prnp*$^{-/-}$ CGNs with 300 μM $CuCl_2$ for 24 h.

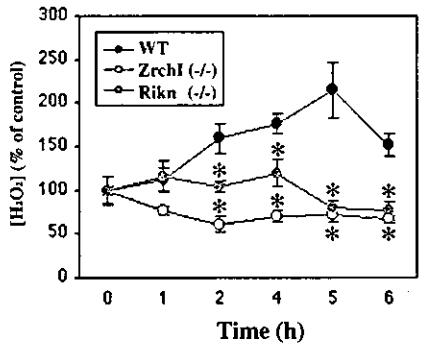

Fig. 3. Evaluation of intracellular H_2O_2 production in WT, ZrchI, and Rikn *Prnp*$^{-/-}$ cerebellar granular neurons (CGNs) after treatments with Cu. WT, ZrchI, and Rikn *Prnp*$^{-/-}$ CGNs were cultured in media containing 300 μM $CuCl_2$ for the indicated time. DCFH-DA was added to the culture medium 30 min after incubation. CGNs collected by pipetting were analyzed by flowcytometry. Intracellular H_2O_2 levels of WT CGNs were increased by Cu, but not those of ZrchI and Rikn *Prnp*$^{-/-}$ CGNs. Differences where $p < 0.05$ (*) were significant when compared with WT CGNs.

than those of ZrchI and Rikn *Prnp*$^{-/-}$ CGNs, suggesting that increase of intracellular H_2O_2 induced by Cu toxicity requires PrP^C expression, and intracellular H_2O_2 in *Prnp*$^{-/-}$ CGNs was effectively converted into hydroxyl radicals by a Fenton reaction. Finally, we investigated the effect of Cu on PrP^C expression in WT CGNs. Flowcytometry revealed that PrP^C expression significantly decreased from cell surface by 6-h exposure of Cu in a dose-dependent manner (Fig. 4).

Accumulating evidence suggests that PrP^C may serve as an antioxidant and/or a Cu-transporting agent. PrP^C has been shown to have an antioxidative and/or anti-apoptotic effect in *Prnp*$^{-/-}$ cell lines [23] and ZrchI *Prnp*$^{-/-}$ neurons [2]. Therefore, we conducted experiments using Rikn *Prnp*$^{-/-}$ mice, which ectopically express PrP-like protein PrPLP/Dpl, [17] to examine whether Rikn *Prnp*$^{-/-}$ neurons are also sensitive to

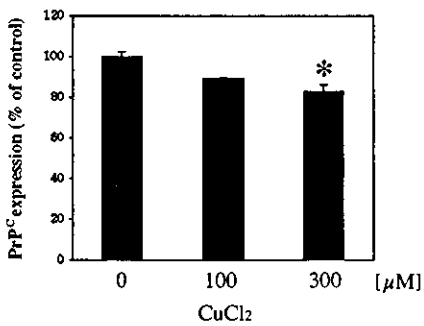

Fig. 4. Decreased expression of PrP^C induced by Cu treatment in WT cerebellar granular neurons (CGNs). PrP^C expression of WT CGNs treated for 6 h with the indicated concentrations of $CuCl_2$ was analyzed by flowcytometry with anti-PrP antibody as described in Materials and methods. Values are expressed as means ± SEM ($N = 3$). Differences where $p < 0.05$ (*) were significant when compared with untreated WT CGNs.

oxidative or apoptotic stress. Rikn *Prnp*$^{-/-}$ CGNs were more susceptible to Cu-induced apoptosis than WT CGNs. There was no difference in viability between WT and Rikn *Prnp*$^{-/-}$ CGNs exposed to any concentration (0, 10, 50, 100, 150, 200, or 300 μM for 48 h) of $ZnCl_2$, $NiCl_2$, or $FeCl_2$ tested (data not shown). Therefore, different from other metals, Cu toxicity on Rikn *Prnp*$^{-/-}$ cells displays a unique perspective.

In this study, Cu-induced oxidative DNA damage and apoptosis in *Prnp*$^{-/-}$ CGNs. The pathways of death signals were investigated to clarify the neuroprotective roles of PrP^C against Cu-promoted apoptosis. Cu induces hydroxyl radicals generated by a Fenton reaction from H_2O_2, resulting in apoptosis [26]. As increase of intracellular H_2O_2 requires PrP^C expression, PrP^C may suppress apoptosis by inhibiting a Fenton reaction and formation of hydroxyl radicals. Decrease of PrP^C expression at cell membrane by Cu is in accordance with a previous report that Cu induces endocytosis of PrP^C [14]. Intracellular PrP^C may have an effect on intracellular H_2O_2 level. Recent studies have reported that Cu toxicity is enhanced by certain oxidants that affect the redox state of Cu. For example, ascorbic acid reduces Cu^{2+} to Cu^+ ion to facilitate ion uptake, thus leading to a loss in cell viability [27]. In cells, L-DOPA, dopamine, and 3-*O*-methyl DOPA inflict extensive oxidative DNA damage in the presence of H_2O_2 and traces of Cu ions [28]. PrP^C-bound Cu is related to the formation of carbonyls by dopamine [29]. Therefore, it is most likely that PrP^C mediates activity of these oxidants via a concurrent dual-action; viz., direct inhibition of the increase in a Fenton reaction coupled with indirect attenuation of the copper toxicity.

Acknowledgments

Thanks are due to Dr. Anthony Foong for reading the manuscript. This work was supported by Grants-in-Aid from the Ministry of Health, Labour and Welfare of Japan (to T.O. and K.S.), a Grant-in-Aid for Scientific Research on Priority Areas (to K.S.), and Grants-in-Aid for Scientific Research (to T.O. and K.S.) from the Ministry of Education, Science, Culture and Technology of Japan. We thank Dr. Stanley B. Prusiner (Institute for Neurodegenerative Disease and Department of Neurology and of Biochemistry and Biophysics, University of California) for providing the original strain of FVB/*Prnp*$^{-/-}$ (ZrchI) mice to breed with C57BL/6 mice.

References

[1] D.R. Brown, J. Sassoon, Copper-dependent functions for the prion protein, Mol. Biotechnol. 22 (2002) 165–178.

[2] D.R. Brown, A. Besinger, Prion protein expression and superoxide dismutase activity, Biochem. J. 334 (Pt. 2) (1998) 423–429.
[3] A.R. White, S.J. Collins, F. Maher, M.F. Jobling, L.R. Stewart, J.M. Thyer, K. Beyreuther, C.L. Masters, R. Cappai, Prion protein-deficient neurons reveal lower glutathione reductase activity and increased susceptibility to hydrogen peroxide toxicity, Am. J. Pathol. 155 (1999) 1723–1730.
[4] D.R. Brown, B. Schmidt, H.A. Kretzschmar, Effects of copper on survival of prion protein knockout neurons and glia, J. Neurochem. 70 (1998) 1686–1693.
[5] C. Kuwahara, A.M. Takeuchi, T. Nishimura, K. Haraguchi, A. Kubosaki, Y. Matsumoto, K. Saeki, T. Yokoyama, S. Itohara, T. Onodera, Prions prevent neuronal cell-line death, Nature 400 (1999) 225–226.
[6] Y. Bounhar, Y. Zhang, C.G. Goodyer, A. LeBlanc, Prion protein protects human neurons against Bax-mediated apoptosis, J. Biol. Chem. 276 (2001) 39145–39149.
[7] C. Atabay, C.M. Cagnoli, E. Kharlamov, M.D. Ikonomovic, H. Manev, Removal of serum from primary cultures of cerebellar granule neurons induces oxidative stress and DNA fragmentation: protection with antioxidants and glutamate receptor antagonists, J. Neurosci. Res. 43 (1996) 465–475.
[8] R.A. Kirkland, J.A. Windelborn, J.M. Kasprzak, J.L. Franklin, A Bax-induced pro-oxidant state is critical for cytochrome *c* release during programmed neuronal death, J. Neurosci. 22 (2002) 6480–6490.
[9] O. Milhavet, H.E. McMahon, W. Rachidi, N. Nishida, S. Katamine, A. Mange, M. Arlotto, D. Casanova, J. Riondel, A. Favier, S. Lehmann, Prion infection impairs the cellular response to oxidative stress, Proc. Natl. Acad. Sci. USA 97 (2000) 13937–13942.
[10] B.S. Wong, T. Pan, T. Liu, R. Li, P. Gambetti, M.S. Sy, Differential contribution of superoxide dismutase activity by prion protein in vivo, Biochem. Biophys. Res. Commun. 273 (2000) 136–139.
[11] F. Klamt, F. Dal-Pizzol, M.J. Conte da Frota, R. Walz, M.E. Andrades, E.G. da Silva, R.R. Brentani, I. Izquierdo, J.C. Fonseca Moreira, Imbalance of antioxidant defense in mice lacking cellular prion protein, Free Radic. Biol. Med. 30 (2001) 1137–1144.
[12] J. Stockel, J. Safar, A.C. Wallace, F.E. Cohen, S.B. Prusiner, Prion protein selectively binds copper(II) ions, Biochemistry 37 (1998) 7185–7193.
[13] M.P. Hornshaw, J.R. McDermott, J.M. Candy, J.H. Lakey, Copper binding to the N-terminal tandem repeat region of mammalian and avian prion protein: structural studies using synthetic peptides, Biochem. Biophys. Res. Commun. 214 (1995) 993–999.
[14] P.C. Pauly, D.A. Harris, Copper stimulates endocytosis of the prion protein, J. Biol. Chem. 273 (1998) 33107–33110.
[15] W. Rachidi, D. Vilette, P. Guiraud, M. Arlotto, J. Riondel, H. Laude, S. Lehmann, A. Favier, Expression of prion protein increases cellular copper binding and antioxidant enzyme activities but not copper delivery, J. Biol. Chem. 278 (2003) 9064–9072.
[16] D.J. Waggoner, B. Drisaldi, T.B. Bartnikas, R.L. Casareno, J.R. Prohaska, J.D. Gitlin, D.A. Harris, Brain copper content and cuproenzyme activity do not vary with prion protein expression level, J. Biol. Chem. 275 (2000) 7455–7458.
[17] A. Sakudo, D.C. Lee, E. Yoshimura, S. Nagasaka, K. Nitta, K. Saeki, Y. Matsumoto, S. Lehmann, S. Itohara, S. Sakaguchi, T. Onodera, Prion protein suppresses perturbation of cellular copper homeostasis under oxidative conditions, Biochem. Biophys. Res. Commun. 313 (2004) 850–855.
[18] D.R. Brown, B.S. Wong, F. Hafiz, C. Clive, S.J. Haswell, I.M. Jones, Normal prion protein has an activity like that of superoxide dismutase, Biochem. J. 344 (Pt. 1) (1999) 1–5.
[19] S.V. Avery, Metal toxicity in yeasts and the role of oxidative stress, Adv. Appl. Microbiol. 49 (2001) 111–142.
[20] H. Bueler, M. Fischer, Y. Lang, H. Bluethmann, H.P. Lipp, S.J. DeArmond, S.B. Prusiner, M. Aguet, C. Weissmann, Normal development and behaviour of mice lacking the neuronal cell-surface PrP protein, Nature 356 (1992) 577–582.
[21] T. Yokoyama, K.M. Kimura, Y. Ushiki, S. Yamada, A. Morooka, T. Nakashiba, T. Sassa, S. Itohara, In vivo conversion of cellular prion protein to pathogenic isoforms, as monitored by conformation-specific antibodies, J. Biol. Chem. 276 (2001) 11265–11271.
[22] A. Sakudo, D.C. Lee, K. Saeki, Y. Nakamura, K. Inoue, Y. Matsumoto, S. Itohara, T. Onodera, Impairment of superoxide dismutase activation by N-terminally truncated prion protein (PrP) in PrP-deficient neuronal cell line, Biochem. Biophys. Res. Commun. 308 (2003) 660–667.
[23] A. Sakudo, D.C. Lee, K. Saeki, Y. Matsumoto, S. Itohara, T. Onodera, Tumor necrosis factor attenuates prion protein-deficient neuronal cell death by increases in anti-apoptotic Bcl-2 family proteins, Biochem. Biophys. Res. Commun. 310 (2003) 725–729.
[24] P.K. Narayanan, E.H. Goodwin, B.E. Lehnert, Alpha particles initiate biological production of superoxide anions and hydrogen peroxide in human cells, Cancer Res. 57 (1997) 3963–3971.
[25] A. Imrich, Y.Y. Ning, L. Kobzik, Intracellular oxidant production and cytokine responses in lung macrophages: evaluation of fluorescent probes, J. Leukoc. Biol. 65 (1999) 499–507.
[26] B. Halliwell, J.M. Gutteridge, Oxygen toxicity, oxygen radicals, transition metals and disease, Biochem. J. 219 (1984) 1–14.
[27] H.J. McArdle, M.J. Bingham, K. Summer, T.J. Ong, Cu metabolism in the liver, Adv. Exp. Med. Biol. 448 (1999) 29–37.
[28] J.P. Spencer, A. Jenner, O.I. Aruoma, P.J. Evans, H. Kaur, D.T. Dexter, P. Jenner, A.J. Lees, D.C. Marsden, B. Halliwell, Intense oxidative DNA damage promoted by L-dopa and its metabolites. Implications for neurodegenerative disease, FEBS Lett. 353 (1994) 246–250.
[29] N. Shiraishi, M. Nishikimi, Carbonyl formation on a copper-bound prion protein fragment, PrP23-98, associated with its dopamine oxidase activity, FEBS Lett. 511 (2002) 118–122.

Available online at www.sciencedirect.com
SCIENCE DIRECT®
Biochemical and Biophysical Research Communications 328 (2005) 1024–1027
BBRC
www.elsevier.com/locate/ybbrc

The N-terminal cleavage site of PrP^{Sc} from BSE differs from that of PrP^{Sc} from scrapie

Hiroko K. Hayashi[a], Takashi Yokoyama[a,*], Masuhiro Takata[a], Yoshifumi Iwamaru[a], Morikazu Imamura[a], Yuko K. Ushiki[a,b], Morikazu Shinagawa[a]

[a] *Prion Disease Research Center, National Institute of Animal Health, 3-1-5 Kannondai, Tsukuba, Ibaraki 305-0856, Japan*
[b] *Nippi Research Institute of Biomatrix, Adachi, Tokyo 120-8601, Japan*

Received 21 December 2004
Available online 25 January 2005

Abstract

Heterogeneity in transmissible spongiform encephalopathy is thought to have derived from conformational variation in an abnormal isoform of the prion protein (PrP^{Sc}). To characterize PrP^{Sc} in bovine spongiform encephalopathy (BSE) and scrapie, we analyzed the newly generated N-terminus of PrP^{Sc} isoforms by digestion with proteinase K (PK). With a lower concentration of PK, the terminal amino acid of BSE PrP^{Sc} converged at N_{96}. Under the same conditions, however, the terminal amino acid of scrapie PrP^{Sc} was G_{81} or G_{85}. Furthermore, with an increase of PK concentration, the N-terminal amino acid was shifted and converged at G_{89}. The results suggest that the PK cleavage site of BSE PrP^{Sc} is uniform and is different from the cleavage site of scrapie PrP^{Sc}.

Keywords: Prion; Scrapie; BSE; PrP^{Sc}; PrPcore; N-terminus

Transmissible spongiform encephalopathies (TSEs) are fatal neurodegenerative disorders. They include scrapie in sheep and goats, bovine spongiform encephalopathy (BSE) in cattle, transmissible mink encephalopathy (TME) in mink, and Creutzfeldt–Jakob disease (CJD) in humans. The infectious agent responsible for these diseases is an abnormal isoform prion protein (PrP^{Sc}), which is thought to be a post-translationally modified form of the host-encoded membrane glycoprotein PrP^{C} [1]. Conversion from PrP^{C} to PrP^{Sc} is thought to be the central event in pathogenesis. The PrP^{Sc} has a large number of β-sheets and a diminished α-helical content as compared with PrP^{C} [2–4]. In addition, PrP^{Sc} is partially resistant to protease digestion; in fact, protease resistance of PrP^{Sc} is a widely accepted physico-chemical test used to distinguish between PrP^{C} and PrP^{Sc}. After treatment with a protease, the amino terminal moiety of PrP^{Sc} is digested and the core fragment (PrPcore), which has an apparent molecular weight of 27–30 kDa, remains [5]. Therefore, usually PrP^{Sc} was detected in protease treated samples as PrPcore by Western blot.

A variety of prion strains exist and they can be distinguished by their different host ranges and by clinical signs, incubation periods, and neuropathology in the brains of mice and hamsters tested with a specific isolate strain of the prion [6–9]. Unfortunately, since transmission studies require a large number of mice and the assay is time consuming, many researchers are working to establish an alternative test with which to differentiate prions with characteristics of PrP^{Sc} [10,11]. Distinct N-termini of PrPcore were observed between different hamster adapted TME isolates [12]. A specifically lower

* Corresponding author. Fax: +81 29 838 7757.
E-mail address: tyoko@affrc.go.jp (T. Yokoyama).

0006-291X/$ - see front matter © 2005 Elsevier Inc. All rights reserved.
doi:10.1016/j.bbrc.2005.01.065

molecular mass of the unglycosylated PrP^{Sc} with BSE prion was also reported [10].

Antibodies that recognize epitopes which locate near the N-terminus of PrPcore are able to distinguish PrP^{Sc} of BSE from that of scrapie [13–15]. However, the exact N-terminus of BSE PrPcore has not been previously determined. Differences in the N-terminus of PrPcore might have resulted from a distinct protein conformation. If so, mapping N-terminus of PrPcore might help to characterize PrP^{Sc} property. Here we report the N-terminal sequence of BSE PrPcore, and its uniformity of cleavage site, which is distinct from the scrapie PrPcore.

Materials and methods

Animals and TSE material. A BSE brain sample from a field case in Japan [16] was homogenized in 9 volumes of phosphate-buffered saline (PBS) and 20 μL each of the homogenate was intracerebrally inoculated into RIII mice (The Jackson Laboratory). Secondary passage of the BSE prion in mice was done by inoculating diseased RIII mouse brain homogenates into RIII and CD-1 mice (SLC/ICR, Japan), and tertiary passage was carried out using CD-1 mice as host and diseased CD-1 mouse brains as inoculum. The Obihiro strain and the Sc237 strain of scrapie prions were inoculated intracerebrally into CD-1 mice and Syrian hamsters, respectively [17].

Purification of proteinase K treated PrP^{Sc} (PrPcore). PrPcore was purified from 1.5 g of brain samples from affected animals as previously described [17]. Briefly, brain samples were homogenized with 10 mM Tris–HCl buffer (pH 7.4) containing 10% Sarkosyl and then centrifuged at 22,000*g* for 10 min. The supernatant was centrifuged at 540,000*g* for 30 min. The resulting pellet was sonicated in Tris–HCl buffer containing 1% Sarkosyl, 10% NaCl (TSN) and centrifuged again at 540,000*g* for 30 min. To obtain the variously PK-treated PrPcore protein samples, the pellets were suspended in TSN, and aliquots were treated with different concentrations of PK (25–800 μg PK/g brain equivalent) at 37 °C for 60 min. The pellets obtained by centrifugation at 22,000*g* for 10 min were washed twice by centrifugation in TSN under the same conditions.

Amino acid sequencing. The PrPcore were subjected to sodium dodecyl sulfate (SDS)–polyacrylamide gel electrophoresis (SDS–PAGE) on a 15% polyacrylamide gel. Proteins fractionated by SDS–PAGE were then transferred electrophoretically to polyvinylidene fluoride membranes (Immobilon PPSQ, Millipore). Proteins on the membranes were stained with coomassie brilliant blue (CBB). The desired protein bands were cut out from the membranes and subjected to amino acid sequencing. N-terminal amino acid sequencing was performed with the HP G1005A Protein Sequencing System (Hewlett–Packard) or with the Procise 494 cLC Protein Sequencing System (PE Biosystems; Apro Science, Tokushima, Japan).

Western blot. Western blot was performed as previously described using anti-prion protein (PrP) mAb T2, and blots were developed with chemiluminescence substrate (Super Signal, Pierce) [18].

Results

Transmission of BSE prion to mice

In order to determine the N-terminal sequence of PrPcore, we first inoculated BSE prion into mice to amplify PrP^{Sc}. BSE was successfully transmitted to all RIII mice with a mean incubation period for the primary BSE passage of 409 days. The incubation period decreased to 221 days (RIII mice) or 196 days (CD-1) mice at the secondary passages. The tertiary passaged mice (CD-1) showed clinical signs and were euthanized at 174 days post inoculation (Table 1).

Table 1
Incubation periods in mice infected with BSE prion

Passage history	Mice	Inoculum	Diseased/ inoculated	Incubation periods[a] (days)
1st	RIII	BSE	5/5	409.0 ± 28.2
2nd	RIII	BSE/RIII	8/8	221.0 ± 4.7
	CD-1	BSE/RIII	21/21	196.8 ± 8.4
3rd	CD-1	BSE/RIII/CD-1	22/22	173.6 ± 7.9

[a] Mean ± SD.

Western blot of PrP^{Sc}

The brains of BSE-affected mice were examined for the presence of PrP^{Sc} at the final stage of the disease. All the mice harbored PrP^{Sc}, though the amounts of PrP^{Sc} in the brain differed at the primary passage. The molecular masses of BSE PrPcore fragments are smaller than those of scrapie, allowing us to distinguish BSE PrP^{Sc} from scrapie PrP^{Sc}. Western blot showed that the profiles of the PrPcore were well conserved throughout the passage history (Fig. 1). In general, the molecular weights of PrPcore fragments in BSE inoculated mice resembled those of PrPcore fragments from BSE-affected cattle, however, di-glycosylated PrPcore in BSE-affected cattle had a larger molecular weight than that in mouse-passaged BSE and that in unglycosylated PrPcore from BSE-affected cattle was somewhat smaller (Fig. 1).

Fig. 1. Western blot of PrP^{Sc} in BSE infected mice. PrPcore was prepared and dissolved in sample buffer. The protein was analyzed by SDS–PAGE, detected with mAb T2. Lane 1, PrP^{Sc} from BSE cattle of 5 mg tissue equivalent. Lane 2, PrP^{Sc} of BSE primary passaged RIII mice. Lane 3, PrP^{Sc} of BSE secondary passaged CD-1 mice. Lane 4, PrP^{Sc} of BSE tertiary passaged CD-1 mice. Lane 5, PrP^{Sc} of Obihiro passaged CD-1 mice. Lanes 2–5, PrP^{Sc} from mouse of 250 μg tissue equivalent. Molecular mass markers are shown on the left (in kiloDalton).

Table 2
Summary of N-terminal sequence of PrPcore of BSE and scrapie

Prion strain/mouse	Proteinase K[a]	Molecular mass[b]	Major sequences	Minor sequence
BSE/RIII/CD-1	25	20	N_{96}	Q_{97}
Obihiro/CD-1	25	21	G_{81}	G_{85}
	130	21	G_{81}, G_{85}, and G_{89}	
	800	21	G_{89}	
Sc237/Syrian hamster	25	21	G_{85} and G_{89}	G_{81}

[a] Amount of proteinase K (μg) for PrP^{Sc} purification with 1 g brain equivalent.
[b] Estimated molecular weight (kDa) from SDS-PAGE.

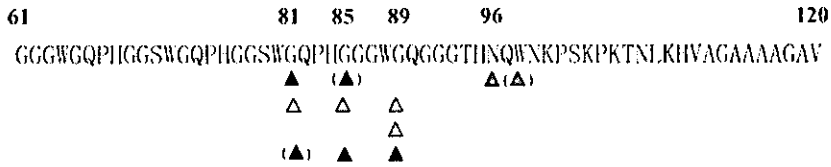

Fig. 2. Proteolysis cleavage sites of PrPcore from BSE and scrapie. N-terminal ends of PrPcore are illustrated. Black triangle, cleavage sites of Obihiro PrPcore with 25 μg/g PK. Yellow triangle, cleavage sites of Obihiro PrP^{Sc} with 130 μg/g PK. White triangle, cleavage site of Obihiro PrP^{Sc} with 800 μg/g PK. Blue triangle, Sc237 PrP^{Sc} with 25 μg/g PK. Red triangle, cleavage sites of BSE PrP^{Sc} with 25 μg/g PK. Minor N-terminal sequences are given in parentheses.

N-terminal amino acid sequence of PrPcore

We next prepared PrPcore from the following animal brains using PK at the concentration of 25 μg/g brain equivalent. The brains from the secondary passage of BSE (BSE/RIII/CD-1), scrapie Obihiro-inoculated CD-1 mice, and scrapie Sc237-inoculated Syrian hamsters were used. As summarized in Table 2, N_{96} was identified as the dominant N-terminal amino acid of BSE PrPcore. In addition, Q_{97} was detected as minor signal. The N-terminus of BSE PrPcore was convergent at N_{96} and Q_{97}, even when treated with a lower concentration of PK. The N-terminus of Obihiro PrPcore in ICR mouse was G_{81} and G_{85}. PrPcore of Sc237 in Syrian hamsters had two dominant terminal amino acids of G_{85} or/and G_{89}, and one minor end at G_{81}.

In order to clear the transition of N-terminus of scrapie PrPcore with different PK concentrations, Obihiro PrPcore was prepared with 130 or 800 μg/g brain equivalent of PK. With 130 μg/mL PK digestion, G_{81}, G_{85}, and G_{89} were identified as N-terminus. There is no significant difference between the proportions of the different fragments. When the Obihiro PrP^{Sc} was treated with 800 μg/mL PK, the terminal amino acid converged at G_{89}. The N-terminus of Obihiro PrPcore remained seven amino acids upstream of that of BSE PrPcore, even with a higher concentration of PK (Table 2 and Fig. 2).

Discussion

To help to understand the molecular basis of PrP^{Sc} characteristics, we analyzed the N-terminal sequence of PrPcore, which was prepared under different conditions. The PK-treated N-terminal amino acid of BSE PrPcore was measured as N_{96} overall, with a small portion of Q_{97}, while that of Obihiro scattered three amino acids of G_{81}, G_{85}, and G_{89}. N-terminal end of BSE PrPcore was 7–15 amino acids apart from that of Obihiro PrPcore (Fig. 2). These data are consistent with our immunoblot result (Fig. 1) and with a previous report [10]. Our results confirm that antibodies that recognize PrP89–95 as an epitope can differentiate BSE and scrapie PrP^{Sc}, as previously reported [15]. Interestingly, the BSE PrP^{Sc} fragment was overwhelmingly convergent to N_{96}, regardless of PK concentration. In contrast, the N-terminal amino acid of Obihiro PrPcore converged to G_{89} with the increasing stringency of PK digestion. Approximate molecular mass difference between the PrPcore of BSE and that of Obihiro was calculated to be 720 and/or 1640 Da. The results also indicate that Obihiro PrPcore has heterogeneity in its cleavage sites. Furthermore, the PK sensitivity of region PrP81–88 is different, in accordance with prion strain variation. Lastly, the results indicate that PrP81–88 of BSE PrP^{Sc} and PrP23–80 might be easily digested with PK, whereas the Obihiro PrP^{Sc} fragment was digested gradually.

That is to say, PrP23–80 seems to be easily digested but the PrP85–88 (GGGW) region is relatively PK resistant, characteristics that were not confirmed in BSE PrP^{Sc}. This subtle difference between the Obihiro and BSE strain PrPcores could not be resolved by SDS-PAGE or immunoblot; detection of the difference requires amino acid sequencing. The PrPcore from Sc237 (hamster) shows cleavage sites similar to those of Obihiro PrP^{Sc} at the middle PK concentration of 130 μg/g. This suggests that accessibility of the N-termi-

nal end of PrPcore differs between the BSE, Obihiro, and Sc237 prions, and that strain-distinct PrP^{Sc} conformation is reflected by this characteristic digestion profile.

The N-terminal ends of PrPcore from ME7 scrapie, TME, and CJD have previously been reported [8,19,20]. The results we obtained with Obihiro and Sc237 were somewhat consistent with previous reports for ME7 and hyper-TME strains. One of the reported N-termini of PrPcore of the drowsy strain of TME (G_{91}, Q_{97}, and K_{100}) overlapped with what we found for BSE PrP^{Sc} [12]. Still, it is not yet clear if a characteristic strain similarity exists between the BSE and drowsy TME prions. Further study will be required to clarify the relationship between PrP^{Sc} conformation, the biochemical and biological properties of PrP^{Sc}, and characteristics of the PrPcore. Mouse-passaged BSE and Obihiro scrapie prions are likely to be a good tool for further investigation.

Acknowledgments

We thank the members of the laboratory facility section in NIAH. We also thank J. Yamada for her general assistance. This study was supported in part by grants from the Ministry of Agriculture, Forestry, and Fisheries, and from the Ministry of Health, Labor, and Welfare.

References

[1] S.B. Prusiner, Molecular biology of prion diseases, Science 252 (1991) 1515–1522.
[2] B.W. Caughey, A. Dong, K.S. Bhat, D. Ernst, S.F. Hayes, W.S. Caughey, Secondary structure analysis of the scrapie-associated protein PrP 27–30 in water by infrared spectroscopy, Biochemistry 30 (1991) 7672–7680.
[3] K.-M. Pan, M. Baldwin, J. Nguyen, M. Gasset, A. Serban, D. Groth, I. Mehlhorn, Z. Huang, R.J. Fletterick, F.E. Cohen, S.B. Prusiner, Conversion of α-helices into β-sheets features in the formation of the scrapie prion proteins, Proc. Natl. Acad. Sci. USA 90 (1993) 10962–10966.
[4] J. Safar, P.P. Roller, D.C. Gajdusek, C.J. Gibbs Jr., Conformational transitions, dissociation, and unfolding of scrapie amyloid (prion) protein, J. Biol. Chem. 268 (1993) 20276–20284.
[5] D.C. Bolton, M.P. McKinley, S.B. Prusiner, Identification of a protein that purifies with the scrapie prion, Science 218 (1982) 1309–1311.
[6] A.G. Dickinson, V.M. Meikle, A comparison of some biological characteristics of the mouse-passaged scrapie agents, 22A and ME7, Genet. Res. 13 (1969) 213–225.
[7] R.I. Carp, S.M. Callahan, E.A. Sersen, R.C. Moretz, Preclinical changes in weight of scrapie-infected mice as a function of scrapie agent-mouse strain combination, Intervirology 21 (1984) 61–69.
[8] R.A. Bessen, R.F. Marsh, Biochemical and physical properties of the prion protein from two strains of the transmissible mink encephalopathy agent, J. Virol. 66 (1992) 2096–2101.
[9] H. Fraser, M.E. Bruce, I. McConnell, Murine scrapie strains, BSE models and genetics, in: R. Bradley, M. Savey, B. Marchant (Eds.), Sub-acute Spongiform Encephalopathies, Kluwer, Dordrecht, 1991, pp. 131–136.
[10] J. Collinge, K.C.L. Sidle, J. Meads, J. Ironside, A.F. Hill, Molecular analysis of prion strain variation and the aetiology of 'new variant' CJD, Nature 383 (1996) 685–690.
[11] J. Hope, S.C.E.R. Wood, C.R. Birkett, A. Chong, M.E. Bruce, D. Cairns, W. Goldmann, N. Hunter, C.J. Bostock, Molecular analysis of ovine prion protein identifies similarities between BSE and an experimental isolate of natural scrapie, CH1641, J. Gen. Virol. 80 (1999) 1–4.
[12] R.A. Bessen, R.F. Marsh, Distinct PrP properties suggest the molecular basis of strain variation in transmissible mink encephalopathy, J. Virol. 68 (1994) 7859–7868.
[13] S. Demart, J.-G. Fournier, C. Creminon, Y. Frobert, F. Lamoury, D. Marce, C. Lasmézas, D. Dormont, J. Grassi, J.-P. Deslys, New insight into abnormal prion protein using monoclonal antibodies, Biochem. Biophys. Res. Commun. 265 (1999) 652–657.
[14] T.G.M. Baron, A.-G. Biacabe, Molecular analysis of the abnormal prion protein during coinfection of mice by bovine spongiform encephalopathy and a scrapie agent, J. Virol. 75 (2001) 107–114.
[15] M.J. Stack, M.J. Chaplin, J. Clark, Differentiation of prion protein glycoforms from naturally occurring sheep scrapie, sheep-passaged scrapie strains (CH1641 and SSBP1), bovine spongiform encephalopathy (BSE) cases and Romney and Cheviot breed sheep experimentally inoculated with BSE using two monoclonal antibodies, Acta Neuropahtol. 104 (2002) 279–286.
[16] K.M. Kimura, M. Haritani, M. Kubo, S. Hayasaka, A. Ikeda, Histopathological and immunohistochemical evaluation of the first case of BSE in Japan, Vet. Rec. 151 (2002) 328–330.
[17] T. Yokoyama, K. Kimura, Y. Tagawa, N. Yuasa, Preparation and characterization of antibodies against mouse prion protein (PrP) peptides, Clin. Diagn. Lab. Immunol. 2 (1995) 172–176.
[18] H. Hayashi, M. Takata, Y. Iwamaru, Y. Ushiki, K.M. Kimura, Y. Tagawa, M. Shinagawa, T. Yokoyama, Effect of tissue deterioration on postmortem BSE diagnosis by immunobiochemical detection of an abnormal isoform of prion protein, J. Vet. Med. Sci. 66 (2004) 515–520.
[19] J. Hope, G. Multhaup, L.J.D. Reekie, R.H. Kimberlin, K. Beyreuther, Molecular pathology of scrapie-associated fibril protein (PrP) in mouse brain affected by the ME7 strain of scrapie, Eur. J. Biochem. 172 (1988) 271–277.
[20] S.G. Chen, W. Zou, P. Parchi, P. Gambetti, PrP^{Sc} typing by N-terminal sequencing and mass spectrometry, Arch. Virol. [Suppl.] 16 (2000) 209–216.

Neuropathology and Applied Neurobiology (2005), **31**, 80–87 doi: 10.1111/j.1365-2990.2004.00592.x

Fatal familial insomnia with an unusual prion protein deposition pattern: an autopsy report with an experimental transmission study

K. Sasaki*, K. Doh-ura*, Y. Wakisaka*, H. Tomodat and T. Iwaki*

**Department of Neuropathology, Neurological Institute, Graduate School of Medical Sciences, Kyushu University, Fukuoka, and †Department of Neurology, Imazu Red Cross Hospital, Imazu, Fukuoka, Japan*

K. Sasaki, K. Doh-ura, Y. Wakisaka, H. Tomoda and T. Iwaki (2005) *Neuropathology and Applied Neurobiology* 31, 80–87

Fatal familial insomnia with an unusual prion protein deposition pattern: an autopsy report with an experimental transmission study

We recently performed a *post-mortem* examination on a Japanese patient who had a prion protein gene mutation responsible for fatal familial insomnia (FFI). The patient initially developed cerebellar ataxia, but finally demonstrated insomnia, hyperkinetic delirium, autonomic signs and myoclonus in the late stage of the illness. Histological examination revealed marked neuronal loss in the thalamus and inferior olivary nucleus; however, prion protein (PrP) deposition was not proved in these lesions by immunohistochemistry. Instead, PrP deposition and spongiform change were both conspicuous within the cerebral cortex, whereas particular PrP deposition was also observed within the cerebellar cortex. The abnormal protease-resistant PrP (PrP^{res}) molecules in the cerebral cortex of this case revealed PrP^{res} type 2 pattern and were compatible with those of FFI cases, but the transmission study demonstrated that a pathogen in this case was different from that in a case with classical FFI. By inoculation with homogenate made from the cerebral cortex, the disease was transmitted to mice, and neuropathological features that were distinguishable from those previously reported were noted. These findings indicate the possibility that a discrete pathogen was involved in the disease in this case. We suggest that not only the genotype of the PrP gene and some other as yet unknown genetic factors, but also the variation in pathogen strains might be responsible for the varying clinical and pathological features of this disease.

Keywords: Creutzfeldt-Jakob disease, NZW mouse, prion disease, thalamic form, transmissible spongiform encephalopathy

Introduction

Fatal familial insomnia (FFI) is one of the disease entities of prion disease or transmissible spongiform encephalopathy (TSE) and it is linked to a mutation at codon 178 of the prion protein gene (PRNP), aspartic acid to asparagine substitution (D178N), in conjunction with methionine at the polymorphic position 129 of the mutant allele [1]. The neuropathological hallmark of FFI is the predominance of lesions within the thalamus [2]. Clinically this disorder is characterized by progressive insomnia, dysautonomia and motor signs [3]. The D178N mutation is also associated with familial Creutzfeldt-Jakob disease (CJD). The disease phenotypes have been considered to depend on the polymorphism at codon 129 of the mutant allele, methionine (129Met) in FFI and valine (129Val) in CJD [4]. However, the FFI genotype reveals diverse clinical expression including cerebellar ataxia, dementia and autonomic abnormalities with or without insomnia [5,6]. In Japan, one FFI case [7] and some cases of the 'sporadic'

Correspondence: Kensuke Sasaki, Department of Neuropathology, Neurological Institute, Graduate School of Medical Sciences, Kyushu University, Fukuoka 812-8582, Japan. Tel: +81-92-6425539; Fax: +81-92-6425540; E-mail: ksasaki@np.med.kyushu-u.ac.jp

thalamic form of CJD [8,9] have been reported, and these have indicated a discrepancy between PRNP genotype and the disease phenotype.

We recently performed a *post-mortem* examination on a Japanese patient with a 27-month history of familial prion disease with PRNP D178N-129Met mutation. The clinical data on this patient and his family have been published in part [10]. Here we report additional clinical data and *post-mortem* neuropathological findings, as well as findings in mice infected with the patient's material.

Case report

The pedigree is presented in Figure 1. In October 1997, a 50-year-old Japanese man (Patient II-5) developed an unsteady gait, followed within a month by difficulty in speech. Although these symptoms worsened rapidly, he did not immediately develop either dementia or insomnia. He was admitted to a hospital for neurological evaluation in February 1998, and PRNP D178N-129Met mutation (heterozygous for 129Met/Val) was revealed as previously reported [10]. From October 1998, either insomnia or delirium was clearly apparent. Hyperthermia without any signs indicative of infection or inflammation, thus suggesting an autonomic sign, was also observed. He often showed reality disturbance and restlessness. He became progressively demented, developed trismus, myoclonus and horizontal nystagmus, and demonstrated increased muscle tone. Finally he became bedridden with flexion contracture. Brain computed tomography revealed mild atrophy of the cerebellum and brainstem. Electroencephalograms showed a background of 9 Hz diffuse α activities, but periodic synchronous discharges were not detected during the clinical course. Sleep activities with rapid eye movements were not recorded in sleep electroencephalograms. In January 2000, he died of pneumonia at the age of 52 years, about 27 months after the onset of disease.

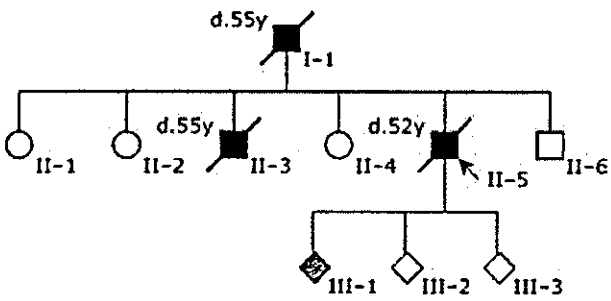

Figure 1. Family tree of the present pedigree. Patients who developed rapidly progressive cerebellar ataxia are depicted by closed symbols, along with their age at death (years old). One of the children of the present case has fatal familial insomnia genotype D178N-129Met/Met (grey symbol).

Patient II-3, one of the brothers of Patient II-5, also showed rapidly progressive cerebellar ataxia. He developed an ataxic gait, forgetfulness and dysarthria at the age of 55 years. Brain computed tomography demonstrated moderate cerebellar atrophy, and electroencephalograms showed diffuse intermittent slow activities without periodic synchronous discharges. He developed myoclonic jerks, akinetic mutism with a decorticate posture, and died 7 months after the onset. Patient I-1, the father of Patients II-5 and II-3, had also developed an ataxic gait and dementia at the age of 55 years. He died of unknown causes after a clinical course of 12 months. Neither autopsy nor PRNP analysis was carried out in either Patient I-1 or Patient II-3. One of the children of Patient II-5 was revealed to have PRNP D178N-129Met mutation (homozygous for 129Met).

Materials and methods

Autopsy was performed 6 h *post-mortem*. A frontal tip of the right cerebral hemisphere and a cerebellar tip were sampled and frozen for Western blot analysis. The remaining brain was immersion-fixed in 10% formalin for 2 weeks. Tissue blocks were immersed in 98% formic acid for 1 h and paraffin-embedded. Hematoxylin and eosin (HE) stain, Klüver-Barrera stain and Bodian's method were performed on 7-μm-thick sections. Immunohistochemical analyses were performed by a standard indirect method for glial fibrillary acidic protein (GFAP) (polyclonal, Dako, Denmark, or monoclonal, clone G-A-5, Roche, Switzerland), ferritin (polyclonal, Dako), β-amyloid precursor protein (APP) (monoclonal, clone LN27, Zymed, USA), SNAP-25 (monoclonal, clone MAB331, Chemicon, USA) and prion protein (PrP) (monoclonal, clone 3F4, Senetek, USA). For anti-PrP immunohistochemistry, sections were pretreated with hydrolytic autoclaving as previously reported [11]. Western blot analysis for protease-resistant PrP (PrP^{res}) was performed using frontal cortical and cerebellar tissue tips from this case, applying phosphotungstic acid precipitation of PrP^{res} as described previously [12] with 50 μg/ml proteinase K (PK) digestion, along with a control case with sporadic

CJD (77-year-old man, duration of illness was 9 months, 129Met/Met). Transmission study was performed as described previously [13]. Briefly, frontal cortical tissue tips were aseptically homogenized with nine volumes of saline, and after removal of debris by low-speed centrifugation the supernatant was used as 10% homogenate. Twenty microliters of 10% homogenate were injected intracerebrally into female NZW mice or female Tg7 mice expressing hamster PrP but not endogenous murine PrP. Sections of infected mice were analysed by HE stain and also by immunohistochemistry for PrP (polyclonal, PrP-C, IBL, Japan) and GFAP (clone G-A-5, Roche). Permission for the animal experiments was obtained from the Animal Experiment Committee of Kyushu University.

Figure 2. Coronal section at the thalamic level. The medial part of the thalamus is atrophic and the third ventricle is dilated.

Results

The brain weighed 1350 g before fixation. The cerebellum showed slight atrophy, whereas the volume of the forebrain was preserved. Coronal sections showed atrophy of the medial part of the thalamus and symmetrical dilatation of the third ventricle (Figure 2).

The summary of histological examination is shown in Figure 3. Marked neuronal loss and moderate astrogliosis in the thalamus were observed, most prominently in its centromedial nucleus and dorsomedial nucleus. However, spongiform change was imperceptible (Figure 4A,B). Neuronal loss and gliosis in the medial portion of the inferior olivary nucleus were also apparent (Figure 4C,D). In the cerebellum there was mild loss of granular cells, and the molecular layer was slightly atrophic. There were localized lesions of spongiosis in the cerebellar molecular layer. Purkinje's cells appeared not to be decreased in number, but they often demonstrated shrunken features. The cerebellar white matter showed diffuse myelin pallor. The cerebral cortex showed uneven distribution of spongiform change and neuronal loss (Figure 4E). There was no apparent difference in the intensities of the cortical lesions among the lobes of the cerebrum except that the lesions are more prominent in the entorhinal cortex and less in the occipital lobe. Moderate astrogliosis was associated with the spongiform lesions (Figure 4F).

Immunohistochemistry for PrP revealed that there was no punctate or plaque-type immunoreactivity in the thal-

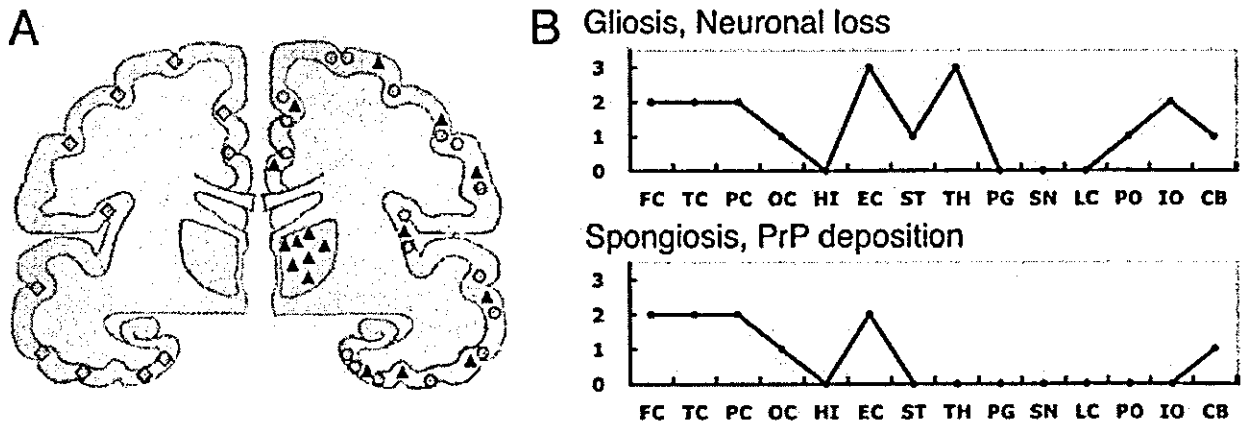

Figure 3. Lesion profiles of the present case. A: schematic drawing of the distribution of prion protein (PrP) deposition (diamonds), spongiosis (circles) and neuronal loss (triangles) in this case, which can be compared to that of fatal familial insomnia (FFI) and 178CJD shown in ref. [19]. B: lesion profiles in respect to gliosis/neuronal loss and spongiosis/PrP deposition. Brain regions studied were: frontal cortex (FC), temporal cortex (TC), parietal cortex (PC), occipital lobe (OC), hippocampus (HI), entorhinal cortex (EC), striatum (ST), thalamus (TH), substantia nigra (SN), periaqueductal grey (PG), pons (PO), locus ceruleus (LC), medulla oblongata (ME), cerebellum (CB). The vertical axis is the degree of lesion graded as follows. 0: not detectable; 1: mild; 2: moderate; 3: severe.

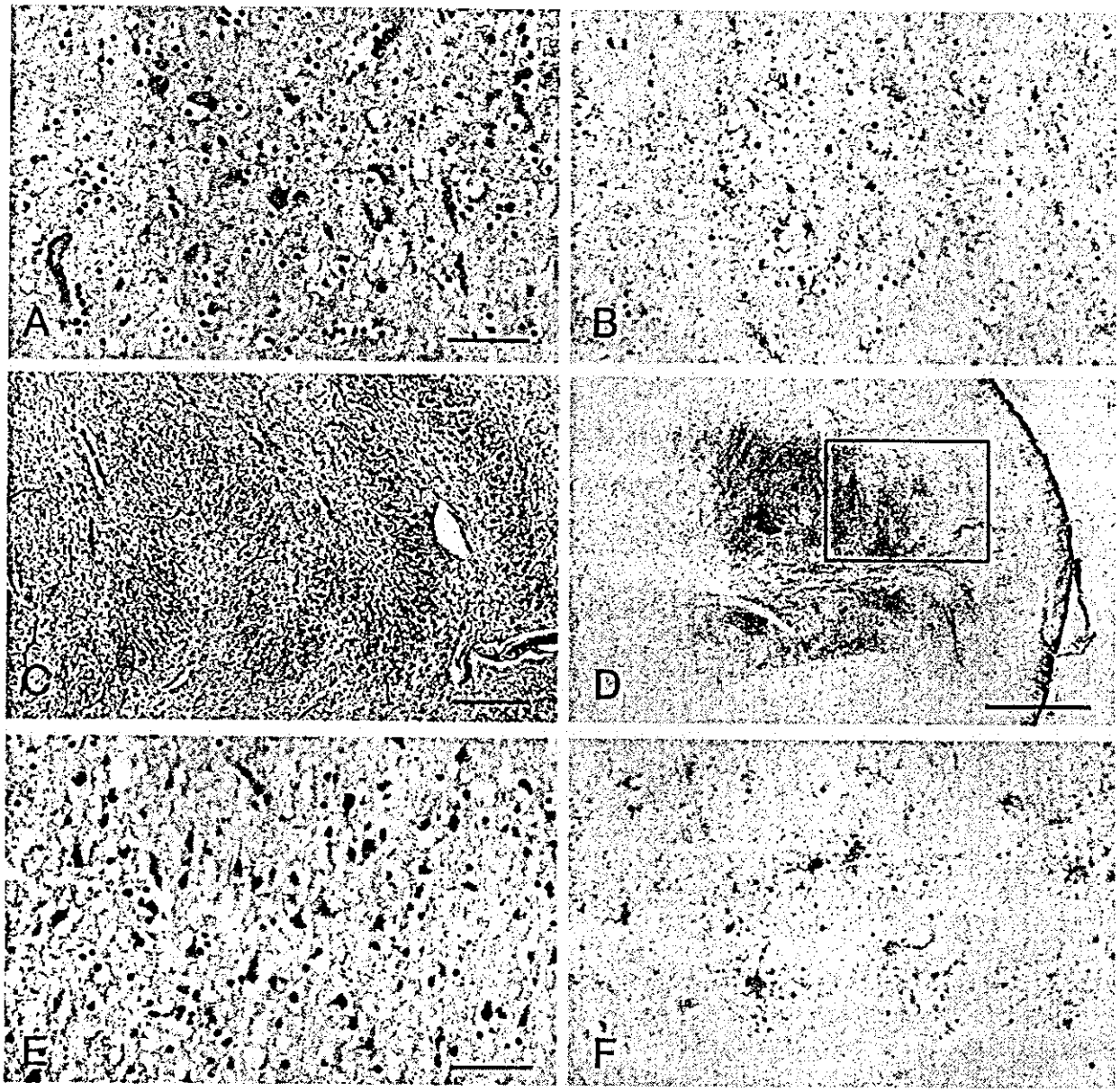

Figure 4. Neuronal loss and gliosis revealed by haematoxylin and eosin stain (A, E), Bodian's stain (C) or immunohistochemistry for glial fibrillary acidic protein (GFAP) (B, D, F). A, B: centromedial nucleus of the thalamus. C, D: inferior olivary nucleus. Neuronal loss is more evident in the medial part (left side of panel C, which represents the rectangular area depicted in panel D). E, F: cerebral cortex (frontal lobe). Both spongiform change and gliosis are remarkable. Bars: 50 μm (A, B, E, F), 200 μm (C), 1 mm (D).

amus or inferior olivary nucleus (Figure 5C,D). In the cerebellar molecular layer, punctate deposits of PrP were focally observed (Figure 5A), and the regions with these deposits were coincident with the extent of spongiform change. Likewise, fine granular deposition of PrP was also detected together with spongiform degeneration in the cerebral cortex (Figure 5B). The distribution of PrP deposits appeared to be more broad and noticeable in the cerebral cortex than in the cerebellum. As a unique finding, the anti-PrP antibody revealed swollen and/or frizzled axons in the deeper parts of the cerebral white matter, in the corpus callosum, or at the borders of the thalamus and caudate nucleus (Figure 5E). Axonal transported substances, APP (Figure 5E, inset) and SNAP-25 (data not shown) were also detected immunohistochemically in those axons.

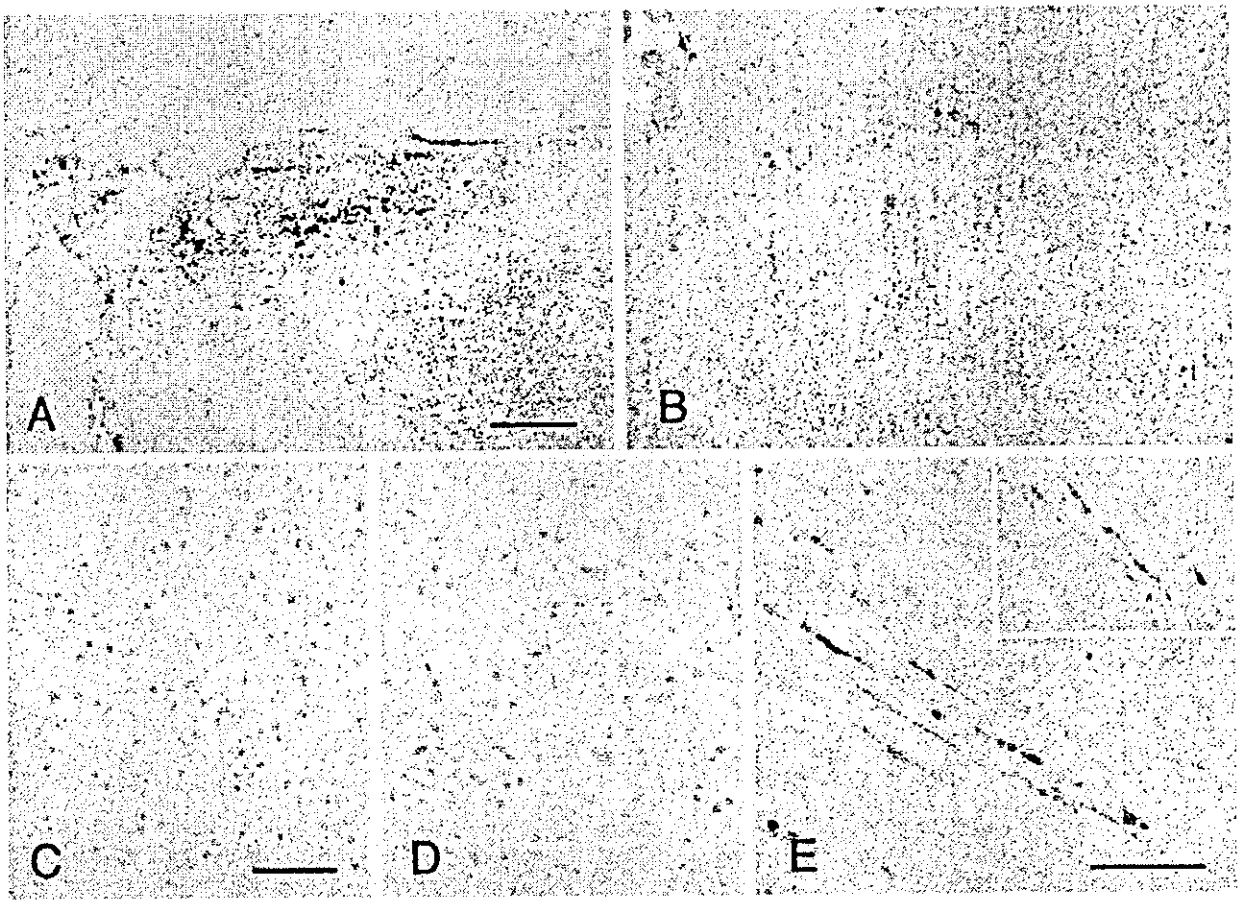

Figure 5. Immunohistochemistry for prion protein (PrP) deposition. A: cerebellum. B: frontal cortex. C: centromedial nucleus of the thalamus. D: inferior olivary nucleus. PrP deposition can not be detected in the thalamus or the inferior olivary nucleus, but coarse or fine granular PrP deposition is visible within the cerebral cortex and the cerebellar molecular layer. E: axons with swollen and/or frizzled features can be detected in the white matter at the border of the thalamus. These axons are also immunostained with anti-APP (amyloid precursor protein) antibody (inset). Bars: 50 μm (A, B, E), 100 μm (C, D).

Although the conventional method of Western blot analysis for PrP^{res} failed to detect any particular signal (data not shown), by application of phosphotungstic acid precipitation that preferably concentrates PrP^{res} but not cellular PrP [12], Western blot analysis of the extract from the frontal cortex of this case revealed a detectable amount of PrP^{res} (Figure 6). The molecular weight of non-glycosylated form of PrP was about 19 kDa (PrP^{res} type 2 pattern) and also the PrP^{res} glycoform ratio was compatible with that of FFI, which has been previously reported [14]. The extract from the cerebellum showed no significant signal in Western blot analysis even with phosphotungstic acid precipitation (data not shown).

The disease of this case was successfully transmitted to some of the mice inoculated with tissue homogenate from the frontal cortex. The incubation time was 571.6 ± 61.1 days (5/7 of the inoculated mice developed TSE) in the NZW mice and 736 ± 64.4 (5/8) in the Tg7 mice, respectively. Although not all the mice developed TSE, diseased mice demonstrated lethargy in the terminal stage rather than excitability. In the TSE-developed mice pathological examination of the brain showed that spongiform change and gliosis were prominent in the cerebral cortex in addition to the thalamus (Figure 7). Immunohistochemistry for PrP revealed that diffuse granular PrP deposition was present within the deep layer of the cerebral cortex as well as in the lateral portion of the thalamus (Figure 7B,E).

Discussion

It is established that there is an overlapping spectrum between classical FFI and CJD in association with PRNP

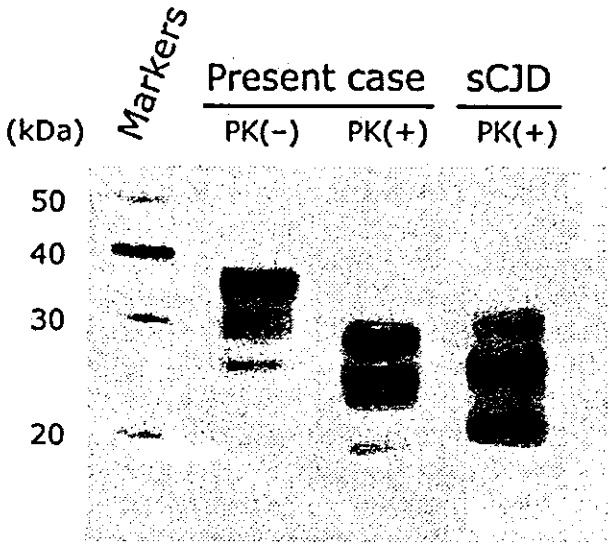

Figure 6. Western blot analysis for protease-resistant prion protein (PrP^{res}). Brain homogenate of the frontal cortex of this case is treated with or without proteinase K (PK), and then PK-digested sample is followed by the 40-times concentration with phosphotungstic acid precipitation for PrP^{res}. The abnormal PrP molecules in the frontal cortex of this case migrate as PrP^{res} type 2. PrP molecules in the lane sporadic Creutzfeldt-Jakob disease (sCJD) are also shown as a standard type 1 PrP (MM1). Molecular sizes (kDa) are indicated on the left.

D178N [6]; however, this case adds to our knowledge about this disease. Although the present case had FFI genotype, the clinical features were initially characterized by prominent cerebellar ataxia, and the neuropathological findings were also atypical in the following respects. First, PrP deposition and spongiform change in the cerebral cortex were more conspicuous than in the thalamus or inferior olivary nucleus, both of which are extremely vulnerable sites for FFI. It has been previously reported that heterozygotes Met/Val at codon 129 result in a longer clinical course than homozygotes [4], and it is therefore possible that the lesions seen in the cerebral cortex were more prominent simply because of the longer course of illness in this patient. However, a further noteworthy point about this case is rather that there was no PrP deposition either in the thalamus or in the inferior olivary nucleus.

Second, immunohistochemical examination detected a peculiar deposition of PrP within the molecular layer of the cerebellum. The localized lesions of granular deposits of PrP and spongiform change in the cerebellar molecular layer seemed to be similar to those reported in a patient from an Austrian FFI family [15]. The cerebellar ataxia of this case could have attributed to the loss of granular neurones and degeneration of Purkinje's cells, in addition to the lesions of the inferior olivary nucleus, although the pathology related to PrP deposition could have also been responsible.

A third atypical feature is that the neuronal loss in the thalamus was most noticeable in the centromedial nucleus. A previous study revealed that severe atrophy of the anterior ventral and dorsomedial thalamic nuclei was consistently observed, whereas that of other thalamic nuclei was less severe and they were inconsistently affected [2]. In this case, the medial portion of the thalamus was indeed damaged crucially, but the principal lesion was different from the typical pathology of FFI.

In addition, an interruption of axonal transport was suggested. Some of the axons were swollen and associated with PrP accumulation, and both APP and SNAP-25 were also accumulated in those axons. APP and SNAP-25 are presynaptic protein and APP is considered as the most effective marker for axonal injury [16]. Aberration in recruitment of PrP might be involved in the pathogenesis of TSE, as described previously [17,18].

This case showed a small amount of specific PrP^{res} in the cerebral cortex but not in the cerebellum as detected by Western blotting. The ratio of PrP^{res} quantity in those regions was visually correlated with that of immunohistochemical reactivity for PrP. Although fresh frozen samples from the thalamus or the inferior olivary nucleus were not obtained for Western blot analyses, we suspect that PrP^{res} in such regions would be too sparse to be detected by Western blotting even in combination with phosphotungstic acid precipitation. The type 2 migration pattern and the glycoform ratio of PrP^{res} in this case were compatible with those in the typical FFI [14]; however, it remains to be elucidated whether these abnormal proteins that can be classified in the same PrP^{res} type may have different influences on the neurodegeneration processes.

Finally, the transmission study revealed that a pathogen in the frontal cortex of this case might be different from that of an FFI case previously reported by Dr Tateishi and his colleagues [13]. NZW mice infected with a thalamic tissue sample of a typical FFI case exhibited excitability as the principal clinical sign and demonstrated PrP deposition predominantly localized within the thalamus. On the other hand, NZW mice infected with a frontal cortical tissue sample from the present case showed lethargy as a clinical sign, and demonstrated diffuse PrP deposition within the deep layer of the cerebral cortex, as well as in the lateral portion of the thalamus. The PrP deposition

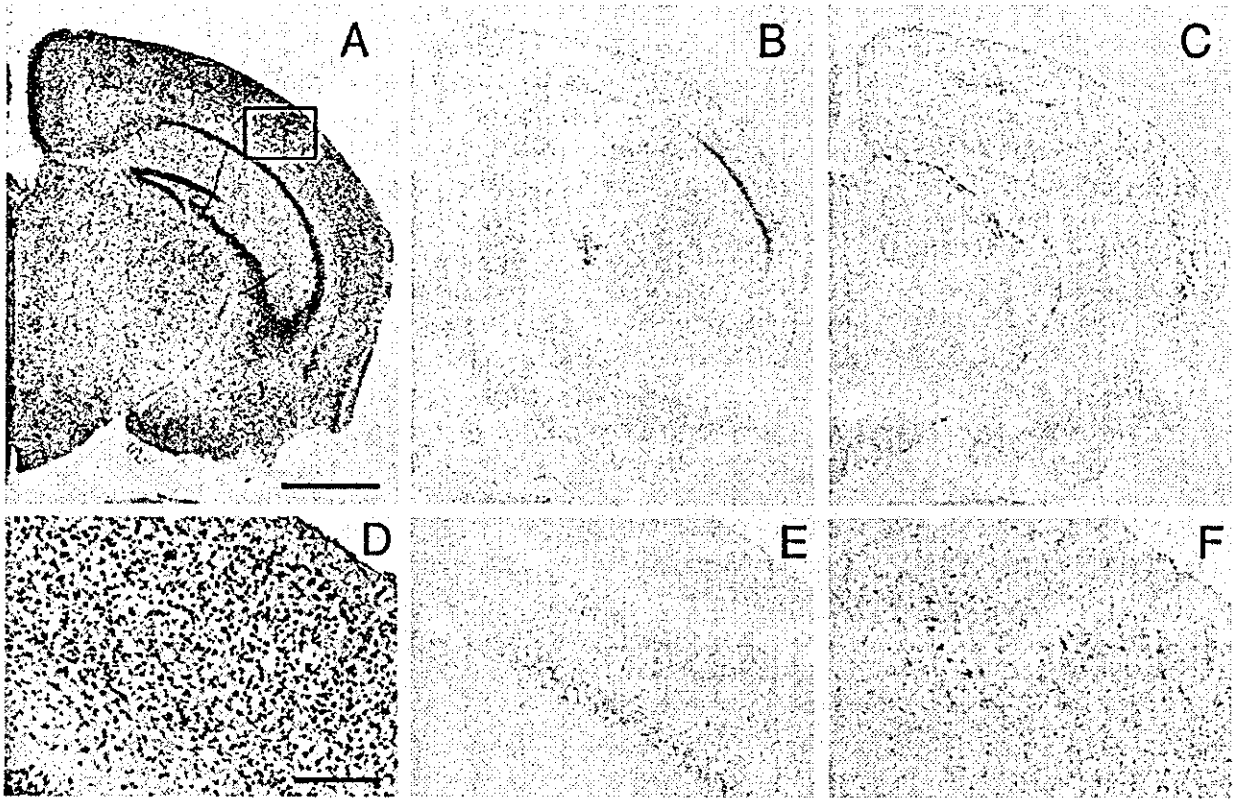

Figure 7. Histological profiles of the mice inoculated with the patient's brain material. A, D: hematoxylin and eosin stain. B, E: prion protein (PrP). C, F: glial fibrillary acidic protein. Spongiform change, PrP deposition and astrocytic gliosis can be observed within the deep layer of the cerebral cortex as well as in the lateral portion of the thalamus. D–F: high power magnifications of the cortical lesions represent the rectangular area depicted in panel A. Bars: 1 mm (A–C), 150 μm (D–E).

pattern of this mouse was distinctive against that of mouse models with other scrapie strains, thus refuting the possibility of contamination. It is not clear whether there were more than two pathogen strains in the brain and whether the strains were dependent on the brain areas. Because we have not examined transmissibility of this case systematically and not obtained frozen materials for Western blot analysis, this aspect still awaits further clarification.

In conclusion, the present case which had FFI genotype showed atypical features, especially with regard to the PrP deposition pattern; there was no deposition within the thalamus or inferior olivary nucleus. Diversity in disease phenotype among patients with the same genotype suggests that some other unidentified factors as well as abnormal PrP deposits or other as yet unknown genetic factors may be responsible for the pathogenesis of the disease. In this study we have shown that variation in pathogen strains may also be one such factor and this factor could have greatly affected the pathogenesis in the present case of FFI.

Acknowledgements

We thank Ms K. Hatanaka for her excellent technical assistance. This study was supported partly by a grant to K. Doh-ura from the Ministry of Health, Labour and Welfare, Japan. Part of this study was carried out at the Morphology Core, Graduate School of Medical Sciences, Kyushu University. The English used in this manuscript was revised by Miss K. Miller (Royal English Language Centre, Fukuoka, Japan).

References

1 Goldfarb LG, Petersen RB, Tabaton M, Brown P, LeBlanc AC, Montagna P, Cortelli P, Julien J, Vital C, Pendelbury WW, Haltia M, Wills PR, Hauw JJ, McKeever PE, Monari L, Schrank B, Swergold GD, Gambetti LA, Gajdusek DC, Lugaresi E, Gambetti P. Fatal familial insomnia and familial Creutzfeldt-Jakob disease: disease phenotype determined by a DNA polymorphism. *Science* 1992; 258: 806–8

2 Manetto V, Medori R, Cortelli P, Montagna P, Tinuper P, Baruzzi A, Rancurel G, Hauw JJ, Vanderhaeghen JJ, Mailleux P, Bugiani O, Tagliavini F, Bouras C, Rizzuto N, Lugaresi E, Gambetti P. Fatal familial insomnia: clinical and pathologic study of five new cases. *Neurology* 1992; 42: 312–9

3 Lugaresi E, Medori R, Montagna P, Baruzzi A, Cortelli P, Lugaresi A, Tinuper P, Zucconi M, Gambetti P. Fatal familial insomnia and dysautonomia with selective degeneration of thalamic nuclei. *N Engl J Med* 1986; 315: 997–1003

4 Parchi P, Petersen RB, Chen SG, Autilio-Gambetti L, Capellari S, Monari L, Cortelli P, Montagna P, Lugaresi E, Gambetti P. Molecular pathology of fatal familial insomnia. *Brain Pathol* 1998; 8: 539–48

5 McLean CA, Storey E, Gardner RJ, Tannenberg AE, Cervenakova L, Brown P. The D178N (cis-129M) 'fatal familial insomnia' mutation associated with diverse clinicopathologic phenotypes in an Australian kindred. *Neurology* 1997; 49: 552–8

6 Zerr I, Giese A, Windl O, Kropp S, Schulz-Schaeffer W, Riedemann C, Skworc K, Bodemer M, Kretzschmar HA, Poser S. Phenotypic variability in fatal familial insomnia (D178N-129M) genotype. *Neurology* 1998; 51: 1398–405

7 Nagayama M, Shinohara Y, Furukawa H, Kitamoto T. Fatal familial insomnia with a mutation at codon 178 of the prion protein gene: first report from Japan. *Neurology* 1996; 47: 1313–6

8 Kawasaki K, Wakabayashi K, Kawakami A, Higuchi M, Kitamoto T, Tsuji S, Takahashi H. Thalamic form of Creutzfeldt-Jakob disease or fatal insomnia? Report of a sporadic case with normal prion protein genotype. *Acta Neuropathol (Berl)* 1997; 93: 317–22

9 Mizusawa H, Ohkoshi N, Sasaki H, Kanazawa I, Nakanishi T. Degeneration of the thalamus and inferior olives associated with spongiform encephalopathy of the cerebral cortex. *Clin Neuropathol* 1988; 7: 81–6

10 Taniwaki Y, Hara H, Doh-Ura K, Murakami I, Tashiro H, Yamasaki T, Shigeto H, Arakawa K, Araki E, Yamada T, Iwaki T, Kira J. Familial Creutzfeldt-Jakob disease with D178N-129M mutation of PRNP presenting as cerebellar ataxia without insomnia. *J Neurol Neurosurg Psychiatry* 2000; 68: 388

11 Sasaki K, Doh-ura K, Ironside JW, Iwaki T. Increased clusterin (apolipoprotein J) expression in human and mouse brains infected with transmissible spongiform encephalopathies. *Acta Neuropathol (Berl)* 2002; 103: 199–208

12 Safar J, Wille H, Itri V, Groth D, Serban H, Torchia M, Cohen FE, Prusiner SB. Eight prion strains have PrP (Sc) molecules with different conformations. *Nat Med* 1998; 4: 1157–65

13 Tateishi J, Brown P, Kitamoto T, Hoque ZM, Roos R, Wollman R, Cervenakova L, Gajdusek DC. First experimental transmission of fatal familial insomnia. *Nature* 1995; 376: 434–5

14 Parchi P, Capellari S, Gambetti P. Intracerebral distribution of the abnormal isoform of the prion protein in sporadic Creutzfeldt-Jakob disease and fatal insomnia. *Microsc Res Tech* 2000; 50: 16–25

15 Almer G, Hainfellner JA, Brucke T, Jellinger K, Kleinert R, Bayer G, Windl O, Kretzschmar HA, Hill A, Sidle K, Collinge J, Budka H. Fatal familial insomnia: a new Austrian family. *Brain* 1999; 122: 5–16

16 Sherriff FE, Bridges LR, Gentleman SM, Sivaloganathan S, Wilson S. Markers of axonal injury in post mortem human brain. *Acta Neuropathol (Berl)* 1994; 88: 433–9

17 Ferrer I, Puig B, Blanco R, Marti E. Prion protein deposition and abnormal synaptic protein expression in the cerebellum in Creutzfeldt-Jakob disease. *Neuroscience* 2000; 97: 715–26

18 Liberski PP, Budka H. Neuroaxonal pathology in Creutzfeldt-Jakob disease. *Acta Neuropathol (Berl)* 1999; 97: 329–34

19 Montagna P, Gambetti P, Cortelli P, Lugaresi E. Familial and sporadic fatal insomnia. *Lancet Neurol* 2003; 2: 167–76

Received 4 February 2004
Accepted after revision 26 April 2004

Available online at www.sciencedirect.com
SCIENCE DIRECT
Biochemical and Biophysical Research Communications 326 (2005) 600–606
BBRC
www.elsevier.com/locate/ybbrc

Octapeptide repeat region and N-terminal half of hydrophobic region of prion protein (PrP) mediate PrP-dependent activation of superoxide dismutase

Akikazu Sakudo[a,b], Deug-chan Lee[a], Takuya Nishimura[a], Shuming Li[b], Shoutaro Tsuji[b], Toyoo Nakamura[c], Yoshitsugu Matsumoto[a], Keiichi Saeki[a], Shigeyoshi Itohara[d], Kazuyoshi Ikuta[b], Takashi Onodera[a,*]

[a] *Department of Molecular Immunology, School of Agricultural and Life Sciences, University of Tokyo, Bunkyo-ku, Tokyo 113-8657, Japan*
[b] *Department of Virology, Research Institute for Microbial Diseases, Osaka University, Yamadaoka, Suita, Osaka 565-0871, Japan*
[c] *Itoham Central Research Institute, Moriya, Kitasoma, Ibaraki 302-01, Japan*
[d] *Laboratory for Behavioral Genetics, Brain Science Institute, RIKEN, Wako, Saitama 351-0198, Japan*

Received 9 November 2004
Available online 7 December 2004

Abstract

Cellular prion protein PrP^C contains two evolutionarily conserved domains among mammals; viz., the octapeptide repeat region (OR; amino acid residue 51–90) and the hydrophobic region (HR; amino acid residue 112–145). Accumulating evidence indicates that PrP^C acts as an inhibitor of apoptosis and regulator of superoxide dismutase (SOD) activity. To further understand how PrP^C activates SOD and prevents apoptosis, we provide evidence here that OR and N-terminal half of HR mediate PrP^C-dependent SOD activation and anti-apoptotic function. Removal of the OR (amino acid residue 53–94) enhances apoptosis and decreases SOD activity. Deletion of the N-terminal half of HR (amino acids residue 95–132) abolishes its ability to activate SOD and to prevent apoptosis, whereas that of the C-terminal half of HR (amino acids residue 124–146) has little if any effect on the anti-apoptotic activity and SOD activation. These data are consistent with a model in which the anti-apoptotic and anti-oxidative function of PrP^C is regulated by not only OR but also the N-terminal half of HR.

Keywords: Prion disease; Prion protein; Apoptosis; PrP-deficient cell line

The spongiform encephalopathies (prion diseases) such as Creutzfeldt–Jakob disease and Gerstmann–Sträussler Scheinker syndrome in humans, scrapie in sheep and goats, and bovine spongiform encephalopathy in cattle are fatal neurodegenerative disorders with pathologies including neuronal cell loss, vacuolation, astrocytosis, and amyloid plaques [1]. The expression of a glycosylphosphatidylinositol (GPI)-anchored plasma membrane cellular prion protein PrP^C is required for the propagation of the prion [2]. Prion infection is attributed to entry of a proteinaceous particle into normal brain, leading to accumulation of an abnormally folded form of the prion protein (PrP^{Sc}) as a consequence of conformational conversion from the endogenous PrP^C [1].

Although several different theories have been proposed, the exact physiological functions of PrP^C remain unclear. Aberrant circadian rhythms [3], electrophysiological abnormalities [4], and high susceptibility to seizure [5] in prion protein (PrP) gene (*Prnp*)-knockout mice have been reported. Furthermore, although several PrP^C binding molecules such as laminin [6], 37-kDa/67-kDa laminin receptor [7], 37-kDa laminin receptor

* Corresponding author. Fax: +81 3 5841 8020.
E-mail address: aonoder@mail.ecc.u-tokyo.ac.jp (T. Onodera).

0006-291X/S - see front matter © 2004 Elsevier Inc. All rights reserved.
doi:10.1016/j.bbrc.2004.11.092

precursor [8], glial fibrillary acidic protein (GFAP) [9], heat shock protein 60 kDa (Hsp60) [10], neural adhesion molecule (N-CAM) [11], Bcl-2 [12], dystroglycan [13], and neuronal isoform of nitric oxide synthase (nNOS) [14] have been reported, the functional significance of the respective bindings remains undefined.

To understand the biological functions of PrP^C, a line of *Prnp*-deficient immortalized hippocampal neuronal cells has therefore been established [15]. Removal of serum from the cell culture causes apoptosis in $Prnp^{-/-}$ cells. Transfection of PrP gene suppresses the apoptosis of $Prnp^{-/-}$ cells under serum-free conditions. These results suggest that PrP^C has an anti-apoptotic function. We have further demonstrated that re-introduction of *Prnp* upregulates superoxide dismutase (SOD) activity and inhibits superoxide generation, suggesting that PrP^C suppresses apoptosis by upregulation of SOD activity [16]. However, PrP^C lacking an octapeptide repeat region (OR) loses its anti-apoptotic function and decreases SOD activity [16]. Brown et al. [17] have reported that the N-terminal OR binds copper and is involved in the SOD-like activity of PrP^C per se. However, it remains unknown whether the crucial role of cellular SOD activity by PrP^C in neuroprotection is a direct result of the enzymatic action of PrP^C or an indirect effect of PrP^C mediating the signals of SOD activation. In support of the latter possibility, several potential mediators of PrP^C signals have been recently reported. Copper specifically binds the OR of PrP^C [18] and enhances endocytosis of PrP^C [19]. A PrP^C-binding molecule, stress-inducible protein 1 (STI1), binds amino acid residue 113–128 located in the N-terminal half of hydrophobic region (HR) of PrP^C and is involved in neuroprotection [20]. These studies prompted us to perform additional studies in order to determine how the OR and HR of PrP^C might contribute to anti-apoptotic and anti-oxidative signals.

To investigate whether the OR and HR are important for the biological activities displayed by PrP^C, several deletion mutants were produced. These mutants were examined for apoptosis-regulating activity as well as SOD-activating action, indicating the importance of the OR and the N-terminal half of HR in anti-apoptotic function and SOD activation. Therefore, we propose that OR and N-terminal half of HR mediate PrP^C-dependent SOD activation that can inhibit apoptosis and may serve as a target in therapies for prion disease.

Materials and methods

Cell cultures and animals. Murine *Prnp*-deficient neuronal cells HpL3-4 [15] and the transfectants including HpL3-4-EM [16], HpL3-4-PrP [16], HpL3-4-Δ#1 [16], HpL3-4-Dpl [21], HpL3-4-Δ#2, and HpL3-4-Δ#3 cells were maintained in Dulbecco's modified Eagle's medium (DMEM) (Sigma, St. Louis, MO) supplemented with 10% fetal calf serum (FCS) at 37 °C in a humidified 5% CO_2 incubator. Unless otherwise specified, serum deprivation was performed as previously described [16].

Plasmid construction and gene transfer. A plasmid containing a *Prnp* cDNA rendering truncated PrPs lacking the HR [PrP(Δ95–132)] or other region [PrP(Δ124–146)] was constructed using the respective restriction enzymes *Hae*II + *Kpn*I or *Ava*II + *Eco*O109I, and a DNA-blunting kit (Takara bio, Otsu, Japan). The *Prnp* deletion cDNAs were subcloned into the multicloning site of internal ribosome entry site (IRES) bicistronic vector pMSCVpuro-EGFP [16]. The resulting constructs pMSCVpuro-PrP(Δ95–132)-EGFP and pMSCVpuro-PrP(Δ124–146)-EGFP, which expressed two genes [enhanced green fluorescent protein (EGFP), and PrP(Δ95–132) or PrP(Δ124–146)] were transiently transfected into the packaging cell line PT67 by the lipofectamine-mediated method (Life Technologies, Gaithersburg, MD). Viral supernatants were harvested for the transduction of HpL3-4 cells. These cells were selected for more than 10 days in 10% FCS-DMEM containing 20 μg/ml puromycin (Wako, Osaka, Japan). Several individual colonies were further selected. The resulting stable *Prnp* deletion cDNA-transfected lines with abundant truncated PrP were used for this study. The resulting stable transfectants were named HpL3-4-Δ#2 and HpL3-4-Δ#3, respectively.

SOD activity assay. Cells were sonicated in ice-cold radio-immunoprecipitation assay (RIPA) buffer supplemented with phenylmethylsulfonyl fluoride and centrifuged at 15,000*g* for 5 min at 4 °C. Protein concentrations of the supernatants were measured by DC protein assay (Bio-Rad). Each protein extract (20 μg) was assayed by SOD assay kit-WST (Dojindo, Kumamoto, Japan). This assay uses the sodium salt of 4-[3-(iodophenyl)-2-(4-nitrophenyl)-2H-5-tetrazolio]-1,3-benzene disulphonate, a water-soluble tetrazolium (WST), as a detector of superoxide radical generation (Peskin and Winterbourn, 2000). The SOD activity was compared with 1 U of bovine erythrocyte Cu/Zn-SOD (Sigma S2515) activity and estimated using the standard curve of SOD activity versus absorbance. The SOD activity was expressed as U/mg protein.

Western blot assay. Western blot assay was performed as described previously [22]. Briefly, cell lysates were prepared in RIPA buffer. The protein concentration was measured using the Bio-Rad DC assay, and SDS/polyacrylamide gel electrophoresis was conducted before electrical transfer onto polyvinylidene difluoride (PVDF) membrane (Hybond-P; Amersham Pharmacia Biotech). PrP was detected as described previously [22] with anti-PrP 6H4 (Prionics, Zürich, Switzerland) [23], anti-PrP P8 [16], anti-PrP SAF32 (SPI bio, Montigny le Bretonneux, France), anti-PrP SAF83 (SPI bio), and anti-Dpl DDC39 [24] or anti-α-tubulin B-5-1-1 (Sigma) and horseradish peroxidase-conjugated secondary antibody. The probed proteins were detected using an enhanced chemiluminescence detection kit (Amersham Pharmacia Biotech).

Cell death assay. Cell death was assessed by measurement of the release of lactate dehydrogenase (LDH) into culture medium, because a loss of cell membrane integrity was observed in dead cells. LDH activity was assayed by the LDH-cytotoxic test (Wako) according to manufacturer's instructions.

Apoptosis assay. DNA fragmentation was detected by the DNA ladder assay [16]. Nuclear morphological analysis was performed by 4′,6-diamido-2-phenylindole hydrochloride (DAPI) staining [22]. Quantitative determination of apoptotic cell death was then performed using a cell death detection enzyme-linked immunosorbent assay (ELISA) kit (Roche Molecular Biochemicals, Indianapolis, IN) according to the manufacturer's instructions. The assay determines the apoptosis index by detecting nucleosome breakdown in the histone-associated DNA fragments (mono- and oligonucleosomes) generated by apoptotic cells and quantifies cell number of apoptotic cells.

Peptide N-glycosidase F digestion. For the cleavage of *N*-glycans, cell lysate was treated with peptide *N*-glycosidase F (PNGase F) (New England Biolabs, Beverly, MA). Protein (60 μg) was denatured at 100 °C for 10 min after addition of 0.1 volume of 10× denaturing buffer (5% SDS, 10% 2-mercaptoethanol). After boiling, 0.1 volume of 10% Nonidet P-40 and 0.1 volume of 0.5 M sodium phosphate buffer (pH

7.5) were added. Aliquots (20 μl) of PNGase F (1 U/μl in 50 mM sodium phosphate buffer, pH 7.5) were added to the reaction mixture and incubated for 2 h at 37 °C. An equal quantity of 2× SDS gel-loading buffer containing 90 mM Tris/HCl (pH 6.8), 10% mercaptoethanol, 2% SDS, 0.02% bromophenol blue, and 20% glycerol was added to terminate the reaction before samples were analysed by Western blotting.

Flow cytometry. Cells were washed twice with PBS and detached using scraper, and then incubated with anti-PrP SAF53 (SPI bio) or SAF61 (SPI bio) for 30 min at 4 °C. Cells were washed with PBS and incubated with phycoerythrin-conjugated secondary antibody (Dako, Copenhagen, Denmark) for an additional 30 min at 4 °C. The expression levels of PrP and deletion mutants were analysed by flow cytometry (FACScan; Becton–Dickinson, San Jose, CA). The data were analysed by Cellquest software (Becton–Dickinson).

Results

From studies on PrP, several regions of PrP have been revealed to be key components. The OR is thought to bind copper and is indispensable for SOD activity of PrP [17,18]. The HR containing the highly conserved sequence motif AGAAAAGA [25] has been shown to be critical to PrP topology in the endoplasmic reticulum membrane [26], normal metabolic cleavage [27], and STI1 binding [20]. The synthetic peptide residues 106–126 of human PrP activate microglial cells which increases their oxygen radical production, mediating a neurotoxicity [28,29]. Furthermore, amino acid sequence comparisons between PrP and PrP homologue PrP-like protein (PrPLP/Dpl) reveal the OR and HR are apparently absent from PrPLP/Dpl [30,31], suggesting that this difference may indicate a significant functional divergence between PrP and PrPLP/Dpl.

To investigate the roles of the OR and HR in anti-apoptotic function of PrP, several deletions were made within these regions of mouse PrP (Fig. 1). The anti-apoptotic function of three PrP deletion constructs was tested following stable transfection into *Prnp*-deficient neuronal cells HpL3-4. We further generated clones of the deletion mutants with levels of expression similar to clones of the full-length protein, as quantitated by Western blot using either anti-PrP SAF32, SAF83 (Fig. 2A), 6H4 or P8 (data not shown). Western blotting with SAF32, which recognizes the 79–92 residues of PrP [32], showed that PrP, PrP(Δ95–132), and PrP(Δ124–146) were detected in HpL3-4-PrP, HpL3-4-Δ#2, and HpL3-4-Δ#3 cells, respectively, whereas SAF32 failed to recognize PrP(Δ53–94, Q52H) in HpL3-4-Δ#1 cells. Western blotting with SAF83, which recognizes the residues 126–164 of PrP [33], indicated that PrP, PrP(Δ53–94, Q52H), and PrP(Δ95–132) were detected in HpL3-4-PrP, HpL3-4-Δ#1, and HpL3-4-Δ#2 cells, respectively, whereas SAF83 failed to recognize PrP(Δ124–146) in HpL3-4-Δ#3 cells. No Dpl was detectable in 60 μg protein of HpL3-4-EM, HpL3-4-PrP, HpL3-4-Δ#1, HpL3-4-Δ#2, and HpL3-4-Δ#3 cells, whereas Dpl was detected in that of HpL3-4-Dpl.

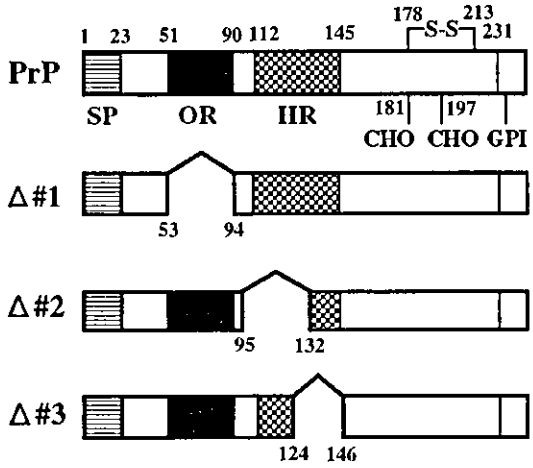

Fig. 1. Schematic presentations of PrP deletion mutants. Mutants of mouse PrP [PrP: wild-type PrP; Δ#1: PrP(Δ53–94, Q52H); Δ#2: PrP(Δ95–132); and Δ#3: PrP(Δ124–146)] were prepared using restriction digestion/ligation. Schematic locations of the deletions as compared with the wild-type protein are shown by a space within the bar next to the indicated protein. Numbers refer to the amino acid residues in the mouse PrP sequence. The disulphides (S–S), two Asn-linked glycosylation sites (CHO), signal peptide sequence (SP), octapeptide repeat region (OR), and hydrophobic region (HR) are shown. PrP has a glycosylphosphatidylinositol (GPI) anchor attached to its C terminus [41].

Equivalent expression levels of PrP and PrP deletion mutants at the cell membrane were also confirmed by cell surface staining with SAF53 and SAF61 using flow cytometry (Fig. 3). PrP is proteolytically cleaved within the HR [34], generating an N-terminally truncated fragment termed PrP-II [35]. After deglycosylation, Western blotting with 6H4, which recognizes residues 144–152 of PrP, demonstrated that full-length PrP and PrP-II were detected in HpL3-4-PrP cells (Fig. 2B). In HpL3-4-Δ#1 cells expressing PrP(Δ53–94, Q52H), which lacks an OR, N-terminally truncated PrP and PrP-II were detected. In HpL3-4-Δ#2 cells expressing PrP(Δ95–132), which lacks an HR, only truncated PrP was detected. Western blotting with P8, which recognizes the 92–109 residues of PrP, demonstrated that only truncated PrP was detected in HpL3-4-Δ#3 cells expressing PrP(Δ124–146). In the absence of serum HpL3-4 cells undergo cell death with features of apoptosis and that transfected $Prnp^{-/-}$ cells with *Prnp* are resistant to serum deprivation [15]. The LDH assay showed that the control transfectants (HpL3-4-EM) underwent cell death rapidly upon serum deprivation, while the full-length PrP-transfected cells were significantly protected (Fig. 4). Similarly, the construct expressing PrP(Δ124–146) demonstrated anti-apoptotic function. In contrast, the cells expressing OR-deficient PrP (HpL3-4-Δ#1) showed reproducible enhancement of cell death compared with HpL3-4-EM cells as already reported [16]. Interestingly, the cells expressing the N-terminal half of HR-deficient PrP (HpL3-4-Δ#2) indicated cell death at equivalent levels